

METAMORPHISM IN THE PALEOPROTEROZOIC TORNGAT OROGEN, LABRADOR: PETROLOGY AND P–T–t PATHS OF AMPHIBOLITE- AND GRANULITE-FACIES ROCKS ACROSS THE KOMAKTORVIK SHEAR ZONE[§]

FLEMMING MENGEL¹

Danish Lithosphere Centre, Østervoldgade 10, DK-1350 Copenhagen K, Denmark

TOBY RIVERS

Department of Earth Sciences, Memorial University of Newfoundland, St. John's, Newfoundland A1B 3X5

ABSTRACT

The Paleoproterozoic Torngat Orogen in northern Labrador developed as a result of collision between the Archean Nain and Southeast Rae cratons. Early phases involved contractional deformation and crustal thickening, whereas later phases were dominated by transcurrent and subsequent near-vertical displacements. The axial region of the orogen is occupied by two major structures, the Abloviak (ASZ) and Komaktorvik (KSZ) shear zones. The gneisses of the Nain Province east of the KSZ are characterized by Archean granulite-facies assemblages; these become progressively overprinted westward by static amphibolite- to granulite-facies assemblages of Paleoproterozoic age toward the KSZ. P–T determinations on the Avayalik dykes and Archean mafic gneisses define a P–T array from *ca.* 11 kbar – 750°C to *ca.* 6 kbar – 600°C. The KSZ is underlain by variably reworked Archean gneisses, mafic and pelitic supracrustal rocks, the Avayalik dykes, anorthosite, and members of the Paleoproterozoic diorite – tonalite – granodiorite (DTG) suite. The peak grade of metamorphism is upper amphibolite to granulite facies; however, P–T determinations from various microstructural settings record a substantial part of the post-peak history. In a range of rock types, an array is defined from *ca.* 11.7 kbar – 720–800°C to *ca.* 6.5 kbar – 540°C. P–T data from west of the KSZ define an array from *ca.* 10 kbar – 786°C to *ca.* 4 kbar – 500°C. In any of the geographic zones above, P–T arrays from each rock type are parallel to the composite array defined by data from all zones. Furthermore, vectors connecting P–T determinations from cores to rims of coexisting minerals are parallel to the overall trend. The data strongly suggest that the Avayalik dykes are most resistant to resetting during cooling, and that mafic orthogneisses, mafic supracrustal rocks and pelitic supracrustal rocks are progressively less robust. Available U–Pb geochronological data suggest that the KSZ and its bordering segments followed different P–T–t paths. From west to east, there is an overall younging in ages of metamorphic zircon, and almost 80 million years of tectonic and metamorphic activity along the KSZ is recorded by ages determined on titanite. The geographic variation in metamorphic ages is interpreted to result from migration of zones where active deformation (and availability of fluid) allowed continued equilibration and growth of metamorphic mineral assemblages.

Keywords: Paleoproterozoic, Torngat Orogen, shear zone, decompression reactions, geothermobarometry, P–T array, geochronology, Labrador.

SOMMAIRE

La ceinture orogénique paléoprotérozoïque de Torngat, dans le nord du Labrador, résulte de la collision entre le socle cratonique archéen de Nain et la partie sud-est du craton de Rae. Les phases précoces ont impliqué un épisode de déformation dû à la contraction et à l'épaississement de la croûte, tandis que des mouvements horizontaux et, plus tard, des mouvements presque verticaux ont dominé les phases tardives. La partie axiale de cette région comprend deux structures, les zones de cisaillement d'Abloviak (ZCA) et de Komaktorvik (ZCK). Les roches gneissiques de la Province de Nain à l'est de ZCK sont des roches archéennes possédant des assemblages typiques du faciès granulite. Ceux-ci se voient progressivement recristallisés vers l'ouest, en direction de la ZCK, par des assemblages de métamorphisme statique dans le faciès amphibolite ou granulite d'âge paléoprotérozoïque. Des déterminations de P et de T faites sur les filons de Avayalik et sur les gneiss mafiques archéens définissent des conditions allant d'environ 11 kbar – 750°C à environ 6 kbar – 600°C. La ZCK est associée à un socle de gneiss archéens et des roches supracrustales mafiques à pélitiques plus ou moins recyclées, des filons de la suite Avayalik, en plus d'anorthosite et de membres d'une suite paléoprotérozoïque à diorite – tonalite – granodiorite (DTG). Le métamorphisme a atteint le faciès amphibolite supérieur à granulite. Toutefois, les déterminations de P et de T provenant de plusieurs milieux

[§] LITHOPROBE contribution number 867.

¹ E-mail address: fcm@dlc.uu.dk

microstructuraux témoignent des conditions largement postérieures au paroxysme métamorphique. Dans une grande variété de roches, les conditions s'étalent entre environ 11.7 kbar – 720–800°C et environ 6.5 kbar – 540°C. Les déterminations de P et de T à l'ouest de la ZCK définissent des conditions entre environ 10 kbar – 786°C et environ 4 kbar – 500°C. Dans chacune des zones géographiques citées, les tracés P–T pour chaque type de roche sont parallèles au tracé composite comprenant toutes nos données pour chacune des zones. De plus, les vecteurs joignant les déterminations du coeur vers la bordure de minéraux coexistants sont parallèles au tracé composite. D'après ces données, les filons de la suite Avayalik semblent les plus résistants au ré-équilibrage pendant le refroidissement, tandis que les orthogneiss mafiques, ainsi que les roches supracrustales mafiques et pélitiques, sont progressivement moins robustes. Les données géochronologiques U–Pb disponibles font penser que la ZCK et les secteurs qui la longent ont subi des évolutions P–T–t différentes. D'ouest en est, il y a un rajeunissement progressif de l'âge du zircon métamorphique, et presque 80 millions d'années d'activité tectonique et métamorphique le long de la ZCK sont indiquées par les âges déterminés sur la titanite. La variation géographique des âges métamorphiques résulterait de la migration des zones de déformation active (et de disponibilité de la phase fluide) qui ont permis un ré-équilibrage et la croissance des assemblages de minéraux métamorphiques.

(Traduit par la Rédaction)

Mots-clés: paléoprotérozoïque, ceinture orogénique de Torngat, zone de cisaillement, réactions de décompression, géothermobarométrie, conditions de P et de T, géochronologie, Labrador.

INTRODUCTION

The estimation of metamorphic conditions places powerful constraints on the tectonic evolution of orogenic belts, especially when used in conjunction with structural and geochronological studies. Since the mid-1970s, when thermal modeling of the orogenic process was first attempted, there has been a viable theoretical framework and reasonable estimates of the principal variables that control the distribution of heat in an active orogen, including thermal conductivities, mantle heat-flow, crustal thickening, uplift and exhumation (e.g., England & Richardson 1977, England & Thompson 1984, Thompson & England 1984, Peacock 1992, Spear 1992, 1994). This theory has been successfully exploited to interpret the tectonic context of pressure (P) – temperature (T) data in many studies of Paleozoic and younger orogenic belts and in a smaller number of studies of older orogenic belts. In the case of deeply eroded Proterozoic orogens, where protoliths of many units are uncertain, mineral assemblages and P–T data may provide essential evidence of many aspects of the tectonic history.

Most orogens preserve evidence of a predominant thrust sense of movement, implying an important early stage of crustal thickening. Many orogens also preserve evidence of a subsequent period of crustal extension correlated with orogenic collapse of the overthickened crust (e.g., Dewey 1988). In deeply eroded orogens, P–T determinations can provide critical evidence to distinguish imbricate stacks formed by thrusting from those formed by extension, and in favorable cases, the calculated P–T differences between adjacent blocks or imbricate slices can be utilised to reconstruct details of the orogenic history (e.g., Hodges & Royden 1984, Spear *et al.* 1984, 1990).

Deeply eroded orogens exhibiting evidence of crustal-scale *transcurrent* motion have received relatively little attention. The Torngat Orogen (Fig. 1) is

characterized by two crustal-scale, ductile transcurrent shear zones that developed following a period of crustal thickening (e.g., Korstgård *et al.* 1987, Mengel & Rivers 1990, Ryan 1990, Van Kranendonk & Ermanovics 1990, Bertrand *et al.* 1993, Rivers *et al.* 1996, Van Kranendonk 1996, Van Kranendonk & Wardle 1996). It is the aim of this study to investigate the P–T–t relationships of the younger Komaktorvik shear zone (KSZ) in the northern part of Torngat Orogen (Fig. 2); the P–T regime of Abloviak shear zone will be the subject of a later study.

P–T DETERMINATIONS IN HIGH-GRADE TERRANES

One of the major potential difficulties associated with the estimation of P and T in granulite- and upper-amphibolite-facies terranes is that the closure temperature of a geothermometer or of a geobarometer may be less than the peak temperature of metamorphism, with the result that the minerals may re-equilibrate on the retrograde path and record a P–T point that is less than the peak conditions attained by the rock (e.g., Frost & Chacko 1989, Harley 1989, Spear & Florence 1992, Pattison & Bégin 1994). This problem has been referred to as the “granulite uncertainty principle” by Frost & Chacko (1989). In addition, if there is non-synchronous closure (“mismatching”: Harley 1989) of the thermometer and barometer, the estimated P–T will be an erroneous point that does not lie on the true P–T–t path (e.g., Selverstone & Chamberlain 1990, Frost & Tracy 1991).

There are no clear-cut ways around these problems, as discussed extensively by the authors noted above, but there are several ways that their effects can be assessed and mitigated.

1) It is essential that the petrographic context of the minerals used for P–T determinations be well established, and the nature and compositions of the neighboring phases be known.

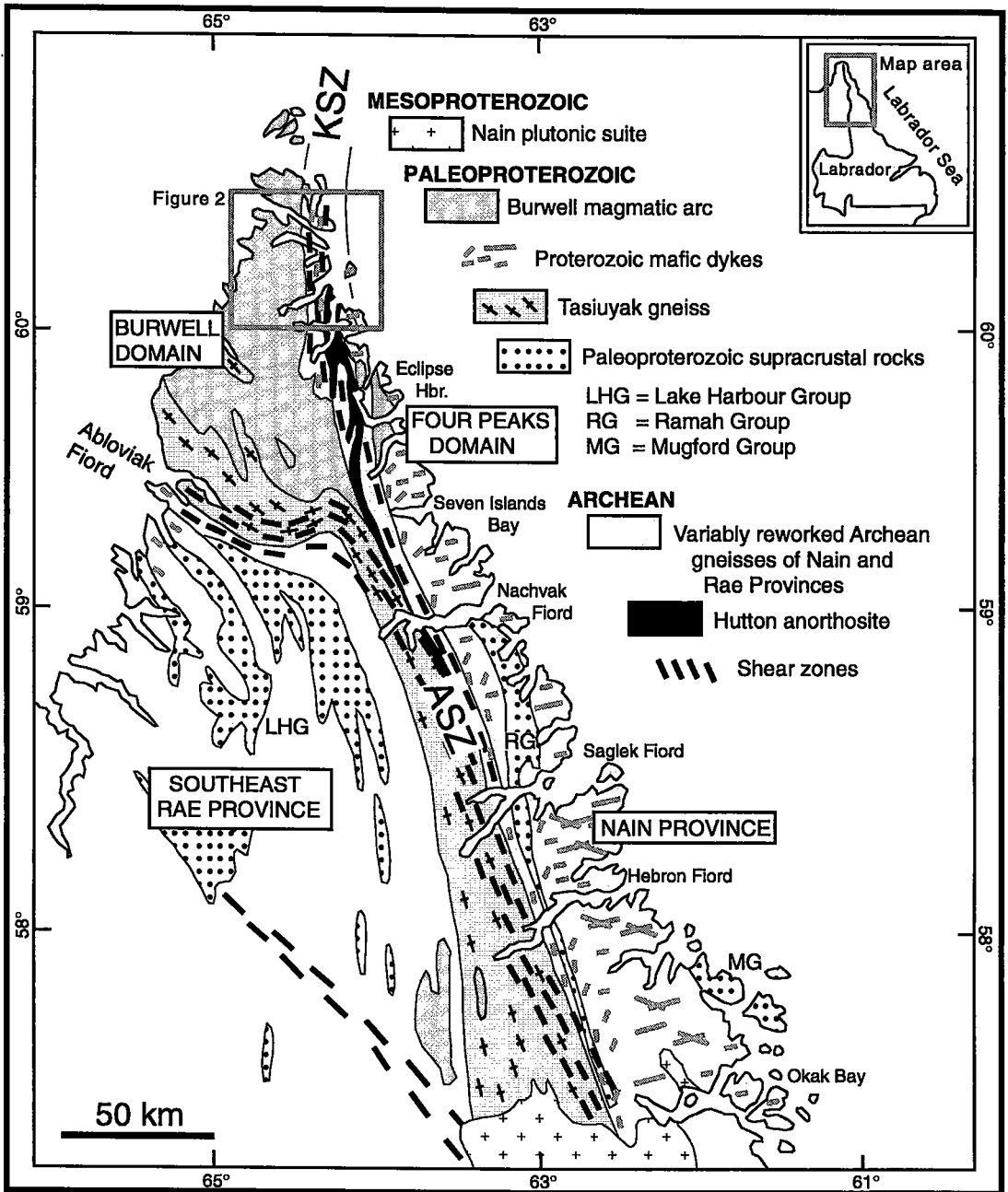


FIG. 1. Overview geological map of the Torngat Orogen, northern Labrador, showing the main lithotectonic elements and geographic locations mentioned in the text (modified from Taylor 1979, Korstgård *et al.* 1987, Van Kranendonk & Ermanovics 1990, Wardle *et al.* 1993, Wardle & Van Kranendonk 1996). "Burwell magmatic arc" includes the DTG and Killinek charnockitic suites.

2) The significance of reaction textures should be evaluated in the context of constraints available from petrogenetic grids. Textures typical of retrograde reactions associated with quasi-isobaric cooling (IBC) and quasi-isothermal decompression (ITD) in granulite-facies rocks have been summarized by Harley (1989) and provide the first clues to the extent and nature of the retrograde path. Although Harley's study was restricted to granulite-facies rocks, equivalent textures must be sought in amphibolite-facies terranes, in addition to petrographic evidence for the prograde or retrograde nature of the amphibolite-facies metamorphism.

3) There is empirical evidence that different samples from a single area and, in some cases, even different textural locations from within a single sample, may record different parts of the P–T path. Such "domainal equilibrium" is the result of variable reaction-progress (controlled by, for example, composition and amount of fluid, bulk composition, deformation) and can conspicuously increase the amount of P–T information from metamorphic rocks if interpreted correctly.

4) Prograde and retrograde reactions, as inferred from textures and constraints from a petrogenetic grid, must be used as qualitative constraints on the slope of the prograde and retrograde portion of the P–T–t path (e.g., Mengel & Rivers 1991).

5) Ideally, several geobarometers should be employed, so that the slope of the P–T–t path can be constrained by various equilibria.

6) Equilibria that are known to close at low temperatures are unlikely to yield realistic estimates of peak P–T conditions. As evidence is accumulated on intracrystalline rates of diffusion of ionic species in a variety of phases, it has become apparent that net-transfer reactions (typical geobarometers) are generally more refractory than exchange reactions (typical geothermometers), such that this constraint is particularly applicable to the latter (e.g., Pattison & Bégin 1994).

In this study, we have worked within these constraints both to provide the best estimates of the high-grade metamorphic conditions recorded in rocks of the KSZ and to define the (prograde and) retrograde part of the P–T path. The limitations of the resultant data-set are discussed below.

TORNGAT OROGEN

Overview

The tectonic setting of the Paleoproterozoic Torngat Orogen (Fig. 1) has been described by several authors (e.g., Korstgård *et al.* 1987, Hoffman 1989, Van Kranendonk *et al.* 1993a, b, Rivers *et al.* 1996, Wardle & Van Kranendonk 1996). The orogen occupies a narrow, north-trending linear belt between the Archean Nain and Southeast Rae provinces, which are

unconformably overlain by the Paleoproterozoic Ramah and Lake Harbour groups, respectively (Jackson & Taylor 1972, Knight & Morgan 1981, Taylor 1979). The western margin of the Nain Craton was strongly reworked in the Torngat Orogen, and there is a steep structural and metamorphic gradient eastward toward the Nain foreland, which consists of unreworked Archean gneisses with a little-deformed Ramah Group cover (Mengel 1988, Van Kranendonk 1996). In contrast, all of the Southeast Rae Craton, its Lake Harbour Group cover and interlayered Paleoproterozoic granitic rocks of the Lac Lomier complex (Ermanovics & Van Kranendonk 1990) were strongly reworked during the Torngat and New Québec orogenies (Bertrand *et al.* 1993, Van Kranendonk *et al.* 1993b).

The axial region of the Torngat Orogen is underlain by a linear belt of strongly deformed, high-grade Paleoproterozoic metasedimentary rocks known as Tasiuyak gneiss (Wardle 1983) that has been interpreted as an accretionary prism covering the suture between the two marginal cratons (e.g., Scott & Campbell 1993, Van Kranendonk *et al.* 1994, Rivers *et al.* 1996).

The eastern margin of northern Torngat Orogen is intruded by a suite of Paleoproterozoic plutons of diorite–tonalite–granite (DTG) composition, whose age, location and composition have been used to infer that the subduction zone was east-dipping, under the Nain Craton, immediately prior to the Torngat Orogeny (Van Kranendonk & Scott 1992, Scott & Campbell 1993, Rivers *et al.* 1996, Van Kranendonk & Wardle 1996).

The northwestern part of the Torngat Orogen, known as Burwell domain (Korstgård *et al.* 1978, Van Kranendonk *et al.* 1993c), is largely underlain by the weakly deformed Paleoproterozoic Killinek charnockitic suite. These calc-alkaline plutonic rocks, which are broadly of the same age and composition as the DGT suite (e.g., Scott 1995b), have been interpreted as representing the root of a continental-margin magmatic arc emplaced into the Nain craton (e.g., Van Kranendonk & Wardle 1994, 1996).

A detailed chronology has been erected for the northern Torngat Orogen based on integrated field and geochronological studies (most recently summarized in, for example, Van Kranendonk & Wardle 1996, in press). Arc magmatism at ca. 1910–1885 Ma was followed by collision and crustal thickening [D_{n+1} ; following Van Kranendonk *et al.* (1993a), all Archean deformation is assigned to D_n] and associated magmatism at 1870–1860 Ma (age data from Bertrand *et al.* 1993, Scott & Machado 1995, Scott 1995a). Subsequently, the Torngat Orogen was dissected by an anastomosing network of crustal-scale, ductile to brittle transcurrent shear-zones up to 15 km wide, of which the largest are the ductile Abloviak and Komaktorvik

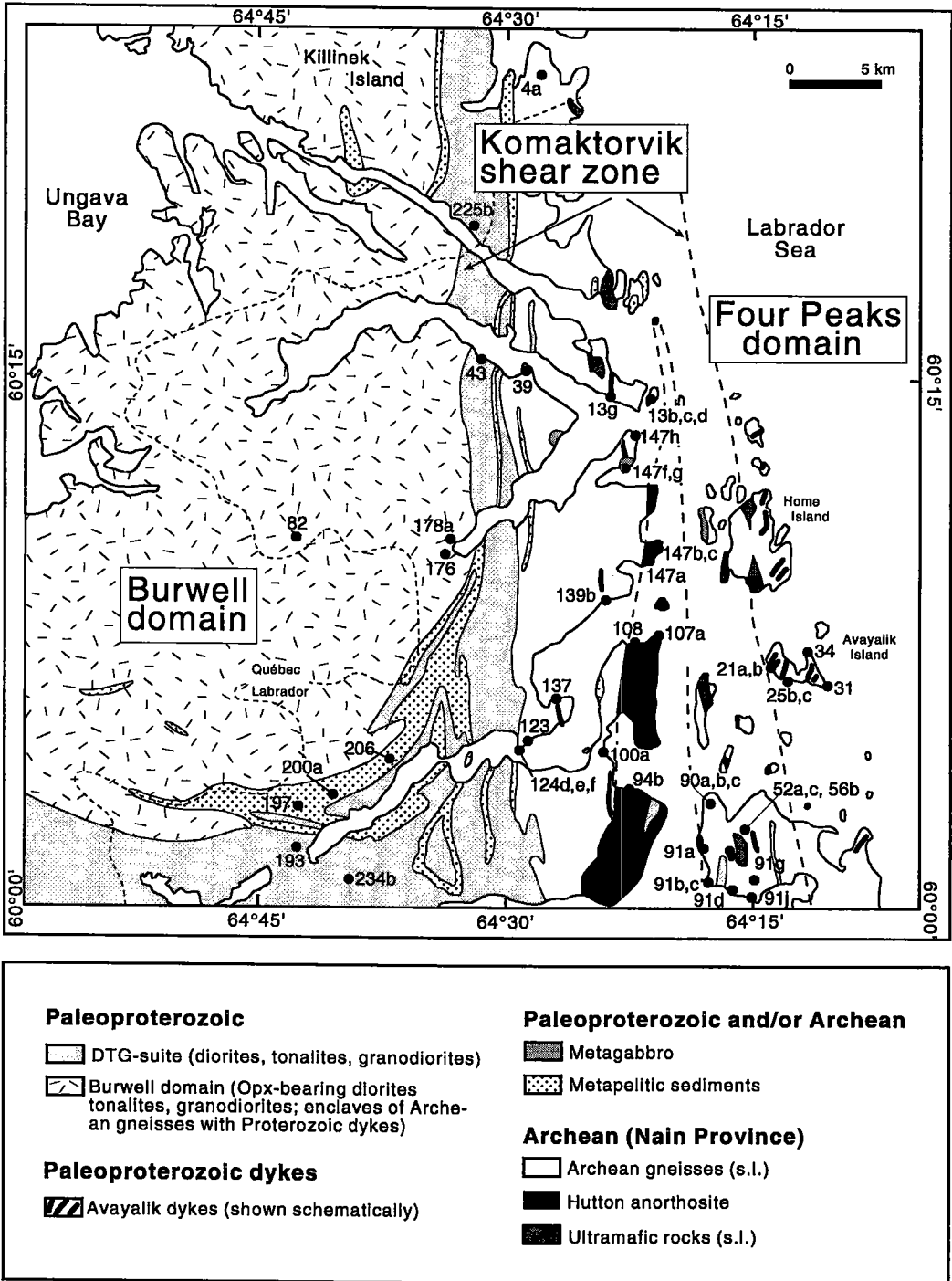


FIG. 2. Simplified geology of the study area in northern Torngat Orogen, showing the main lithological units and the location of the samples investigated. The position of the Komaktorvik shear zone is taken from Wardle *et al.* (1993); see Van Kranendonk & Wardle (1996) for more details. Modified from Wardle *et al.* (1993).

shear zones (Fig. 1). The Abloviak shear zone (ASZ), a sinistral, transpressional D_{n+2} structure formed at 1845–1822 Ma (Bertrand *et al.* 1993), is principally developed in Tasiuyak gneiss and reworked gneisses of the Southeast Rae craton. The younger Komaktorvik shear zone (KSZ) is a D_{n+3} structure that was mainly active *ca.* 1798–1780 Ma (Bertrand *et al.* 1993, Van Kranendonk *et al.* 1994, Scott & Machado 1995, Van Kranendonk & Wardle 1996, in press) and that affected reworked gneisses of the Nain Craton and the Paleoproterozoic DTG suite. In the northern part of the orogen, the two shear zones are separated by the Burwell domain, whereas farther south, the Komaktorvik zone (as defined in Van Kranendonk *et al.* 1993c) dies out at *ca.* 59° latitude (Fig. 1).

Northern Torngat Orogen

The geology of the northern part of Torngat Orogen adjacent to the Komaktorvik shear zone is shown in more detail in Figure 2 (from Wardle *et al.* 1993). For the purposes of this study, the area has been subdivided into three north–south-trending segments centered on the Komaktorvik shear zone. The main features of the geology in each zone in the studied cross-section are as follows.

The *Four Peaks domain*, east of the Komaktorvik shear zone, is underlain principally by an Archean basement gneiss complex consisting of tonalitic to granodioritic gneiss with rafts of Archean pelitic and basic supracrustal rocks, cross-cut by the undeformed Paleoproterozoic Avayalik dykes (Wardle *et al.* 1992, 1993). This area is part of the structural foreland of the Torngat Orogen, but both dykes and gneisses have been affected by a static Paleoproterozoic, granulite- to amphibolite-facies metamorphic overprint (Morgan & Taylor 1972, Mengel & Rivers 1994, Van Kranendonk *et al.* 1994, Wardle *et al.* 1994, Connelly & Mengel 1995, Van Kranendonk & Wardle 1996) (see below).

The *Komaktorvik shear zone* is underlain by reworked Archean gneisses, the isoclinally folded, late Archean(?) Hutton anorthositic suite (defined in Van Kranendonk *et al.* 1993c) and by Paleoproterozoic dykes, metasediments and DTG suite intrusions. The pronounced structural grain of the zone is a result of penetrative, broadly north-striking, steeply dipping LS fabrics that are mylonitic to locally ultramylonitic in character (Van Kranendonk *et al.* 1993a). Most high-strain zones are narrow, discontinuous features, suggesting that strain was localized in progressively narrower zones, and that overall displacement was limited (*e.g.*, Van Kranendonk & Wardle 1996). Stretching lineations in the shear fabric, defined by amphibolite-facies mineral assemblages, are of two dominant generations. The older generation is broadly south-plunging and associated with oblique, sinistral, east-side-up movements (*i.e.*, D_{n+3}). The younger D_{n+4}

lineations are down-dip, and occur in ultramylonites associated with later west-side-up movements (Van Kranendonk *et al.* 1993a, 1994, Van Kranendonk & Wardle 1994). The earlier structures have been interpreted to indicate an overall scissor movement on the Komaktorvik shear zone, with increased east-side-up displacement toward the north (Van Kranendonk & Wardle 1996, in press).

Most rocks in the Komaktorvik shear zone are of amphibolite-facies grade, but there is widespread evidence in mafic orthogneisses and supracrustal rocks for earlier granulite-facies metamorphism (Grt–Cpx–Pl and Grt–Opx–Pl assemblages). Since it occurs in the DTG suite and Avayalik dykes, this episode of metamorphism must be Paleoproterozoic in age. Note that mineral abbreviations, unless otherwise noted, are from Kretz (1983).

The *Burwell domain*, west of the Komaktorvik shear zone, is dominated by the Killinek charnockitic batholith, with some pelitic rocks (some of which are similar to the Tasiuyak gneiss) occurring around the margins and structurally on top of the batholith (Van Kranendonk & Wardle 1996). The intrusive rocks are variably foliated and lineated, and contain granulite-facies metamorphic mineral assemblages. In the eastern part of the batholith, adjacent to the Komaktorvik shear zone, fabrics are oriented north–south. Farther west, these D_{n+1} foliations are folded into NW-plunging D_{n+2} structures (Van Kranendonk *et al.* 1994). Throughout its outcrop area, the Killinek charnockite contains numerous enclaves (m to km scale) of folded Archean gneisses with discordant mafic dykes. These enclaves have been tentatively linked to the Four Peaks domain by Van Kranendonk *et al.* (1994) and Connelly & Mengel (1995), whereas reconnaissance Pb-isotopic data (Campbell *et al.* 1995) show greater similarities to gneisses of the Rae Province. Thus their affiliation is presently uncertain.

METAMORPHISM IN TORNGAT OROGEN

Previous studies of metamorphism in the Torngat Orogen

There have been several studies of the metamorphic development of Torngat Orogen in the last few years. Previous work by the authors (Mengel 1988, Mengel & Rivers 1990, 1991, 1992, 1994) was concerned with the metamorphic development of Torngat Orogen along an E–W transect at the latitude of Saglek Fiord, extending from the foreland (Ramah Group) to the interior (ASZ). Van Kranendonk (1992, 1996) reported results from a parallel transect at the latitude of Okak Bay (Fig. 1).

The metamorphic signature along Saglek Fiord (Fig. 1) was first examined by Mengel & Rivers (1990,

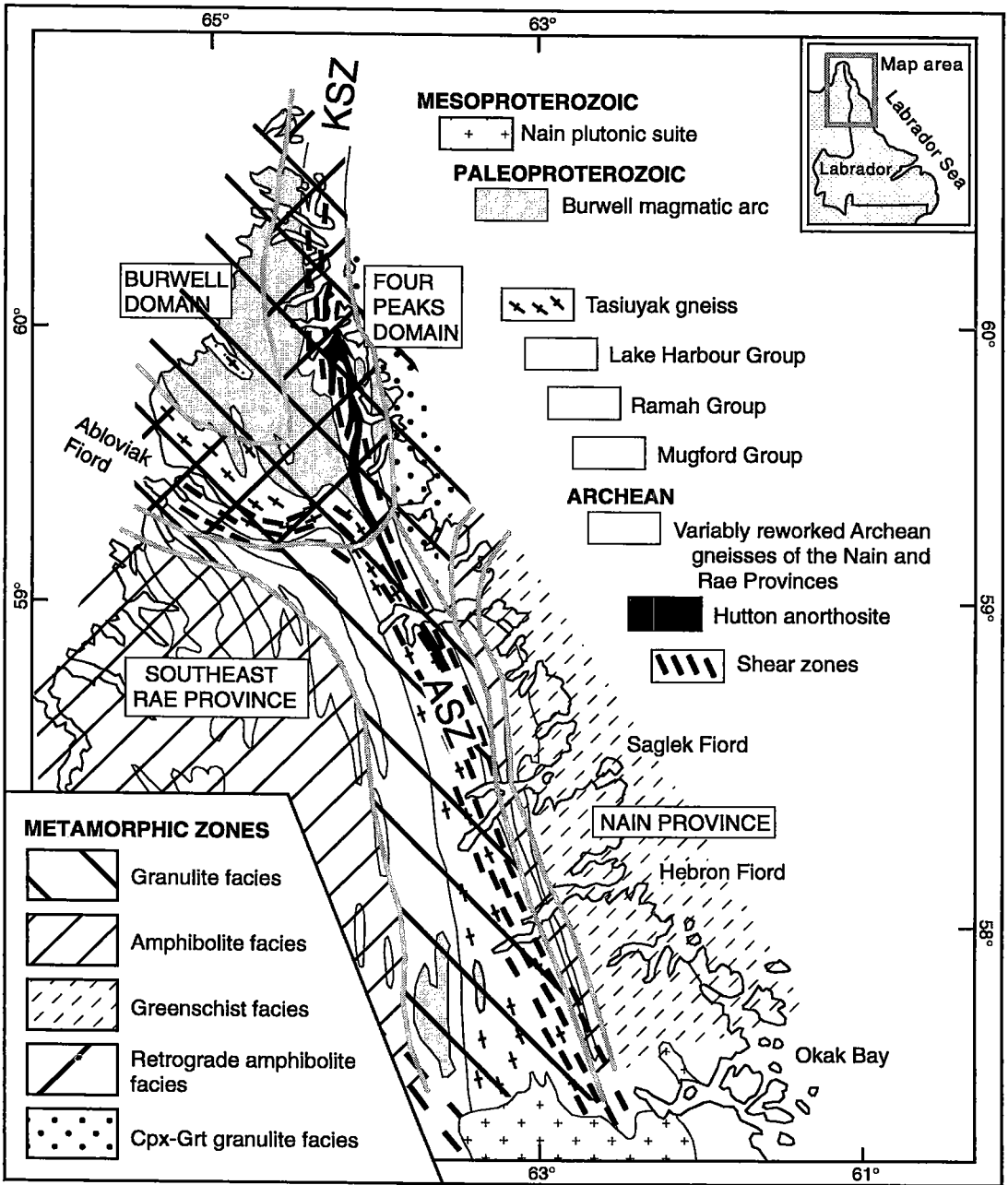


FIG. 3. Schematic extent of Paleoproterozoic metamorphic zones in the Torngat Orogen, including data from Wardle *et al.* (1994), Wardle & Van Kranendonk (1996), Van Kranendonk & Wardle (1996, 1997) and Van Kranendonk & Mengel (1996). The base map is identical to that in Figure 1. The patterns for the Lake Harbour, Ramah and Mugford Groups have been omitted for clarity.

1991), who subdivided the ASZ into distinct granulite- and upper-amphibolite facies slices that were juxtaposed during late (*i.e.*, post-transcurrent shearing) east-directed thrusting [D_3 of Van Kranendonk & Ermanovics (1990), Stage 3 of Bertrand *et al.* (1993)]. Using samples of mafic rocks from both these slices (their amphibolite- and granulite-facies blocks, respectively), Mengel & Rivers (1990, 1991) defined a P–T path constrained by concordant P–T vectors from both individual samples and the sample population as a whole, indicating a quasi-ITD path in this part of the ASZ from *ca.* 10 kbar – 800°C to *ca.* 5 kbar – 650°C.

There have been several interim reports of ongoing metamorphic studies in and adjacent to the Komaktorvik shear zone in the northern part of the orogen (*e.g.*, Mengel & Rivers 1992, 1993, Patey 1994, 1995, Mengel *et al.* 1996). In these communications, the authors provided preliminary P–T results, and discussed the nature of mineral reactions and their relationship to transcurrent shearing. It is our aim in this paper to summarize these results, present some new data, and integrate the resultant data-set with available geochronological and structural constraints.

Regional distribution of metamorphic rocks

Figure 3 shows the regional distribution of metamorphic grade in the northern Torngat Orogen. In general, metamorphic grade increases toward the axial region of the orogen, where it attains the uppermost amphibolite to granulite facies. Metamorphic orthopyroxene is widespread in iron-rich tonalites and basic lithologies, whereas the highest-grade assemblages in pelites display the association Grt – Bt – Sil – Pl – Kfs – Qtz.

At the latitude of Saglek Fiord, the across-strike distribution of metamorphic grade is well displayed. Here, there is a progressive increase in metamorphic grade westward from the greenschist facies at the Torngat Front (defined as the easternmost Paleoproterozoic thrust, *e.g.*, Mengel 1988, Van Kranendonk 1990, Van Kranendonk *et al.* 1993c) toward upper-amphibolite to granulite-facies assemblages in the central part of the orogen, resulting in the familiar telescoped pattern of “inverted” metamorphic zones seen in many orogens with a predominant thrust-sense of displacement. However, in the northern part of the orogen, the structural and metamorphic fronts of the orogen diverge, and, as noted above, there is a static upper-amphibolite- to granulite-facies metamorphic overprint well to the east of the Komaktorvik shear zone (Morgan & Taylor 1972), which on structural grounds marks the eastern boundary of the orogen at this latitude (Van Kranendonk & Mengel 1996, Wardle & Van Kranendonk 1996).

West of the Komaktorvik shear zone, foliated intrusive rocks of the Killinek charnockitic batholith

exhibit variably retrograde granulite-facies mineral assemblages, and reworked gneisses of the Southeast Rae Province basement, south and west of the Abloviak shear zone, similarly show widespread evidence of an amphibolite-facies retrogression of earlier granulite-facies assemblages of unknown age.

Age of metamorphism

Available geochronological data on Paleoproterozoic metamorphism in and adjacent to the Komaktorvik shear zone from the northern part of the orogen are summarized in Table 1 and Figure 4. The age determinations have been grouped in the three segments defined above, *i.e.*, (1) Four Peaks domain east of the KSZ, (2) Komaktorvik shear zone (including the Hutton anorthositic suite), and (3) the Burwell domain west of the KSZ.

TABLE 1. PALEOPROTEROZOIC METAMORPHISM IN THE TORNGAT OROGEN, NORTHERN LABRADOR: SELECTED GEOCHRONOLOGICAL DATA

| Age | Mineral | Rock type | Source |
|-------------------------------------|-------------|----------------------------------|--------|
| Burwell Domain | | | |
| 1745 ± 2 Ma | Ttn | gneissic tonalite | (1) |
| 1767 ± 4 | Ttn | diorite | (1) |
| 1776 ± 2 | Ttn | tonalite | (1) |
| 1814 | Mnz | felsic gneiss | (2) |
| 1814 | Zrn | felsic gneiss | (2) |
| 1843 ± 3 | Zrn | charnockite | (1) |
| 1843 | Zrn | mafic dyke | (2) |
| 1871 ± 3 | Zrn | charnockite | (1) |
| 1877 | Zrn | mafic gneiss | (2) |
| Komaktorvik Shear Zone | | | |
| 1710 ± 4 Ma | Ttn | diorite | (1) |
| 1720 | Ttn | | (2) |
| 1735 ± 3 | Ttn | dioritic dyke | (1) |
| 1745 ± 3 | Ttn | in 2.8 Ga tonalite | (1) |
| 1748 ± 3 | Zrn | gabbro anorthosite | (1) |
| 1751 ± 4 | Ttn | tonalite | (1) |
| 1774 ± 3 | Ttn | granitic vein | (1) |
| 1780 ± 2 | Zrn and Mnz | interboudin pegmatite | (1) |
| 1780 ± 3 | Zrn | Hutton anorthositic suite | (1) |
| 1781 ± 2 | Zrn | Hutton anorthositic suite | (1) |
| 1789 ± 1 | Zrn | synkinematic pegmatite | (1) |
| 1791 ± 2 | Zrn | granite | (1) |
| 1793 | Zrn | mafic gneiss | (2) |
| 1800 | Zrn | mafic gneiss | (2) |
| Nain Province | | | |
| 1719 ± 2 Ma | Zrn | synkinematic pegmatite | (1) |
| 1740 +8/-4 | Zrn | Avayalik dyke | (1) |
| 1743 | Zrn | Avayalik dyke | (2) |
| 1834 +7/-3 | Zrn | Avayalik dyke | (1) |
| Southern Torngat Orogen (TO) | | | |
| 1730–1740 Ma | Hbl | Ar–Ar data from southern TO | (3) |
| 1750–1790 | Hbl | Ar–Ar data from southern TO | (4) |
| 1740–1795 | Zrn and Mnz | D_3 uplift along ASZ | (4) |
| 1822–1845 | Zrn | D_3 deformation – metamorphism | (1,4) |
| 1866–1860 | Zrn | D_1 deformation – metamorphism | (1,4) |

Mineral symbols are those of Kretz (1983). Sources of data: (1): Scott & Machado (1995), Scott (1995a,b), (2): Connelly & Mengel (1995, 1996), (3): Mengel *et al.* (1991), (4): Bertrand *et al.* (1993).

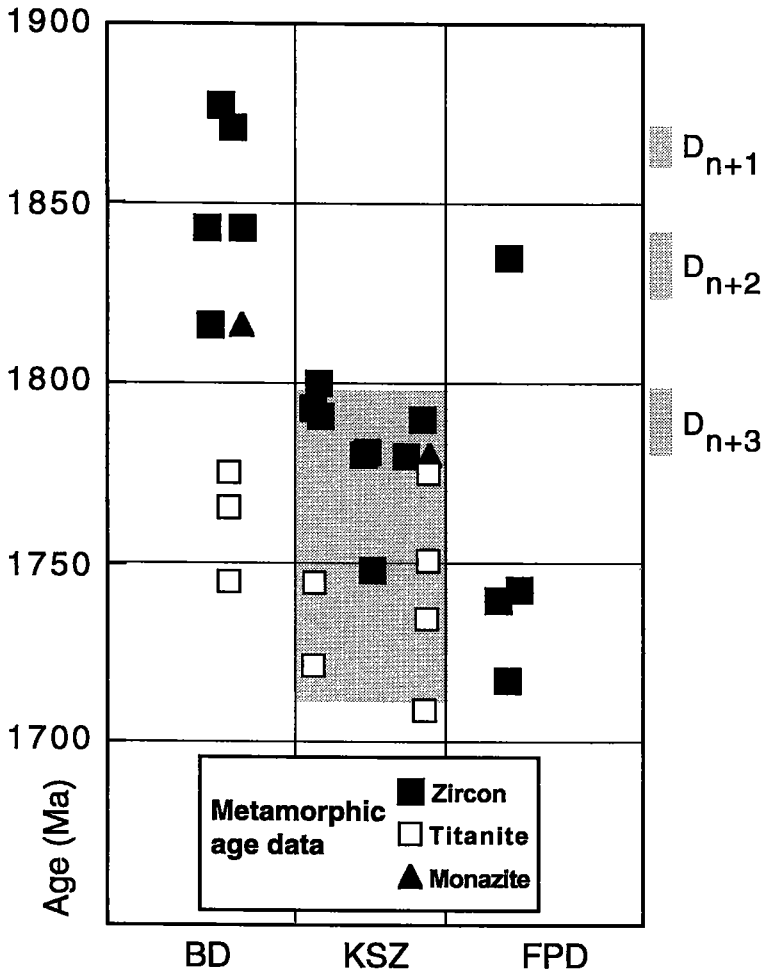


FIG. 4. Summary of metamorphic age data (in Ma) from the northern Torngat Orogen, compiled from Scott (1995a, b), Scott & Machado (1995), Connelly & Mengel (1995, 1996). Gray shading in the Komaktorvik shear zone (KSZ) covers the range of metamorphic and synkinematic ages obtained by Scott & Machado (1995). Samples from the western KSZ are shown schematically on the left side of the KSZ field, and data for the eastern KSZ are on the right side. Samples within the Burwell domain (BD) and the Four Peaks domains (FPD) are not arranged geographically. Sources of data are given in Table 1. Bars labeled D_{n+1} , D_{n+2} and D_{n+3} represent the main tectonic phases recognized in the northern Torngat Orogen (references above and in text).

The data show several groups of ages based on metamorphic zircon: *ca.* 1875 Ma, 1843 Ma and 1816 Ma in Burwell domain, *ca.* 1795 Ma, 1775 Ma and 1750 Ma in the KSZ, and 1834 Ma, *ca.* 1740 Ma and 1719 Ma in the Four Peaks domain. The youngest generation of metamorphic zircon closed to Pb loss at 1816 Ma in the Burwell domain, at 1748 Ma in

the KSZ, and at 1719 Ma in the Four Peaks domain. A similar, although less pronounced variation is shown by the ages based on titanite, which range from 1775 to 1745 Ma in the Burwell domain and from *ca.* 1775 to 1710 Ma in the KSZ.

The available Ar/Ar cooling ages for hornblende from the area between Saglek Fiord and Okak Bay

TABLE 2. SUMMARY OF ROCK TYPES AND MINERAL ASSEMBLAGES

TABLE 2 (continued)

| Sample | Rock type | 1 | 2 | 3 | 4 | 5 | 6 | Others |
|---|--|---|---|---|---|---|---|-----------------------|
| Four Peaks domain (east of Komaktorvik shear zone) | | | | | | | | |
| 21a | Grt-rich mafic granulite | | x | | x | | | Opq |
| 25b | Grt-Cpx-rich layer in supraxx sequence | x | x | x | | x | | Opq |
| 31 | P dyke, Grt-bearing | x | x | x | x | | | Cal, Kfs |
| 21b | Grt-Cpx mafic gneiss | | x | | x | | | |
| 25c | Grt-Bt-rich layer in supraxx sequence | x | x | | | x | | Zrn |
| 34 | Anorthosite from mafic layered complex | | x | x | x | | | Opq |
| Eastern Komaktorvik shear zone | | | | | | | | |
| 52a | Grt-Hbl gneiss | | x | | x | | | Opq |
| 52c | P dyke, Grt-bearing | | x | | x | | | Opq, Ep |
| 90a | Leucocratic Grt amphibolite | | x | x | x | | | |
| 90b | Grt-Cpx amphibolite | | x | | x | | | |
| 90c | Grt-Hbl-Pl layer in amphibolite | | x | x | x | | | Opq |
| 91b | Grt amphibolite (metagabbro) | | x | x | x | | | Cal |
| 91g | Grt-Sil-bearing metapelite | | x | | | | x | Rt, Zrn, Opq, Ep |
| 91j | Grt-Hbl-bearing metasediment | | x | | x | | | Rt, Ep, Cal, Cum, Opq |
| 56b | Layered charnockite - mafic tonalite | | x | x | x | | | Ap |
| 91d | Mylonite with Grt-Pl clasts | | x | | | x | | |
| Central Komaktorvik shear zone (Hutton anorthositic suite) | | | | | | | | |
| 91a | Grt mylonite layer in Anorthosite | | x | | x | | | |
| 94b | Grt-Cpx-bearing mafic supracrustal rock | | x | x | x | | | Ttn |
| 107a | Grt-Cpx mafic gneiss | | x | x | | | | Ttn, Ilm, Mag |
| 108 | Grt-Cpx mafic gneiss | | x | x | x | | | Ep, Cal, Ilm |
| 147b | Grt-Opx-Hbl layer in anorthositic gneiss | | x | | x | | | Cal, Ilm |
| 91c | Grt-Opx gneiss from UM sequence | | x | x | x | | | Ap |
| 147a | Grt-Hbl-bearing anorthositic gneiss | | x | | x | | | Ep, Rt |
| Western Komaktorvik shear zone | | | | | | | | |
| 4a | Grt-Hbl-bearing mafic supracrustal rock | | x | | | x | | Opq |
| 13b | Grt-bearing metapelite | | x | | | x | x | Opq |
| 13c | Grt-bearing mafic supracrustal rock | | x | x | | | | Cal, Ttn |
| 39 | Grt-bearing layered mafic granulite | | x | x | x | | | Ap, Opq |
| 100a | Grt-Cpx mafic granulite | | x | x | x | | | |
| 124d | Grt-Bt-Sil metapelite | | x | | | x | x | |
| 139b | P dyke, Grt-rich | | x | | x | x | | Zrn, Opq, Cal, Ep |
| 147f | Grt-Hbl-bearing gabbro | | x | | x | x | | Ap |
| 147g | P dyke, Grt-bearing dyke cutting 147f | | x | x | x | | | Cal, Opq |
| 147h | P dyke, Grt-bearing dyke cutting 147f | | x | x | x | | | |
| 13d | Grt-bearing mylonitic metapelite | | x | | | x | x | |
| 13g | P dyke, Grt amphibolite | | x | x | x | | | Cal, Opq |
| 123 | Mylonitic Grt-Bt-bearing metapelite | | x | | | x | | Zrn |
| 124e | Grt-Bt-Sil metapelite schist | | x | | | x | x | Chl, Kfs |
| 124f | Grt-Bt-Hbl mafic schist | | x | | | x | x | Ttn, Ms |
| 137 | P dyke, Pl-phyruc, Grt-bearing | | x | x | x | | | Cal, Ep, Chl, Ap |
| Burwell domain (west of Komaktorvik shear zone) | | | | | | | | |
| 43 | Sheared gabbroic rock | | x | x | x | | | Opq |
| 197 | Grt-Bt-Sil metapelite, supraxx sequence | | x | | | x | x | Opq, Zrn, Kfs |
| 200a | Grt amphibolite, supracrustal sequence | | x | x | x | | | Zrn, Ap |
| 234b | Grt-Cpx granulite in Opx gneiss | | x | x | x | | | Ilm |
| 82 | Charnockite <i>sensu lato</i> | | x | x | | | | Ap, Opq, Zrn |
| 176 | Charnockite <i>sensu lato</i> | | x | x | x | | | Opq, Kfs |
| 178a | Charnockite <i>sensu lato</i> | | x | x | x | | | Kfs |
| 193 | Tonalite-granodiorite | | x | x | x | | | Opq, Ap |
| 206 | Tonalite-granodiorite | | x | x | x | | | Cal, Ilm |
| 225b | Tonalite-granodiorite | | x | x | x | | | Opq, Ap |

Columns headings: 1 garnet, 2 orthopyroxene, 3 clinopyroxene, 4 hornblende, 5 biotite, 6 sillimanite. The mineral symbols used are those of Kretz (1983), except that Opq represents the opaque minerals. Abbreviations: "supraxx" = supracrustal, UM = ultramafic, P = Proterozoic. Sample numbers in bold-face type: samples were used in thermobarometric calculations. Sample numbers shown in italics: samples were not used for thermobarometry. Note that all samples contain quartz and plagioclase.

(Fig. 1) are in the range 1790–1730 Ma (Mengel *et al.* 1991, Bertrand *et al.* 1993) and overlap with titanite ages in the KSZ from the northern part of the orogen (1774–1710 Ma, Fig. 4, Table 1), which implies that amphibolite-facies fabrics in the orogen developed over a period of ca. 80 My.

Sample selection

For the present study, samples were chosen to represent the full east-west width of the northern Komaktorvik shear zone and to extend into the adjacent Four Peaks and Burwell domains (Fig. 2, Table 2). Inasmuch as permitted by the distribution of lithologies, an attempt was made to sample Archean mafic gneisses, mafic and pelitic supracrustal rocks, and Proterozoic mafic dykes across the area of interest. Locally, members of the Proterozoic DTG suite and some bodies of gabbro also were sampled in order to complete the sample distribution. Sampling was designed (1) to estimate the P-T conditions during shearing along the Komaktorvik shear zone, (2) to test whether there is a systematic variation of

Paleoproterozoic metamorphic grade along the length of this part of the shear zone, (3) to determine if metamorphic grades of narrow, structurally later high-strain zones differ from the main part of the KSZ, and (4) to provide a metamorphic evaluation of the hypothesis, defined on structural grounds, that the shear zone underwent east-side-up movement (Van Kranendonk & Scott 1992, Van Kranendonk & Wardle 1994, 1996).

The majority of the samples of Archean mafic supracrustal rocks and Proterozoic mafic dykes contain one or more of the following assemblages: Grt - Hbl - Pl - Qtz, Grt - Cpx - Pl - Qtz, Grt - Opx - Pl - Qtz. A few samples lack garnet, but contain the assemblage Opx - Cpx - Hbl - Pl - Qtz. Samples of the pelitic supracrustal rocks contain the assemblage Grt - Bt - Pl - Sil - Qtz - (\pm Rt - Ilm). Table 3 shows selected compositions of the minerals used for thermobarometry. The complete set of analytical data is available from the first author and from the Depository of Unpublished Data, CISTI, National Research Council, Ottawa, Ontario, Canada K1A 0S2.

TABLE 3. REPRESENTATIVE MINERAL COMPOSITIONS

| Sample Mineral Code | 31 | | | 52c | | | 91a | | | 39 | | | 234b | | |
|--------------------------------|-------|-------|-------|--------|-------|-------|-------|-------|-------|--------|-------|--------|-------|-------|--------|
| | Grt | Hbl | Pl | Grt | Hbl | Pl | Grt | Hbl | Pl | Grt | Hbl | Pl | Grt | Hbl | Pl |
| SiO ₂ wt% | 37.47 | 41.87 | 59.52 | 38.15 | 40.19 | 60.98 | 38.05 | 41.42 | 57.69 | 37.97 | 42.36 | 60.30 | 37.60 | 41.32 | 56.17 |
| TiO ₂ | 0.01 | 1.09 | 0.01 | 0.01 | 0.76 | 0.01 | 0.01 | 0.98 | 0.01 | 0.01 | 1.53 | 0.01 | 0.01 | 2.12 | 0.01 |
| Al ₂ O ₃ | 21.15 | 13.41 | 24.14 | 21.55 | 14.82 | 24.24 | 21.53 | 14.39 | 25.51 | 20.52 | 12.92 | 25.53 | 21.31 | 12.37 | 27.70 |
| Cr ₂ O ₃ | 0.04 | 0.01 | 0.07 | 0.09 | 0.01 | 0.01 | 0.09 | 0.04 | 0.01 | 0.01 | 0.02 | 0.02 | 0.01 | 0.04 | 0.04 |
| FeO | 29.07 | 15.47 | 0.41 | 26.89 | 19.15 | 0.24 | 26.34 | 13.59 | 0.01 | 29.14 | 17.78 | 0.01 | 28.69 | 17.70 | 0.16 |
| MnO | 1.24 | 0.01 | 0.01 | 2.31 | 0.20 | 0.01 | 0.72 | 0.01 | 0.01 | 2.87 | 0.20 | 0.20 | 1.06 | 0.01 | 0.01 |
| MgO | 3.31 | 9.77 | 0.16 | 2.29 | 7.43 | 0.01 | 6.63 | 10.38 | 0.01 | 3.88 | 8.80 | 0.01 | 3.58 | 8.41 | 0.01 |
| CaO | 7.17 | 11.34 | 6.14 | 10.36 | 11.33 | 5.29 | 5.14 | 11.28 | 6.98 | 6.71 | 11.37 | 6.92 | 7.49 | 11.39 | 9.76 |
| Na ₂ O | 0.35 | 1.92 | 8.22 | 0.05 | 2.00 | 8.78 | 0.01 | 1.69 | 7.77 | 0.06 | 2.04 | 9.12 | 0.01 | 1.94 | 9.67 |
| K ₂ O | 0.01 | 1.84 | 0.21 | 0.13 | 1.35 | 0.01 | 0.01 | 1.11 | 0.10 | 0.07 | 1.36 | 0.01 | 0.01 | 1.58 | 0.07 |
| Sum | 99.82 | 96.73 | 98.89 | 101.83 | 97.24 | 99.58 | 98.53 | 94.89 | 98.10 | 101.24 | 98.38 | 102.13 | 99.77 | 96.88 | 103.60 |

| Sample Mineral Code | 13c | | | 25b | | | 25b | | | 91g | | | 124d | | |
|--------------------------------|--------|-------|-------|-------|-------|-------|-------|-------|-------|--------|-------|-------|--------|-------|-------|
| | Grt | Cpx | Pl | Grt | Cpx | Pl | Grt | Opx | Pl | Grt | Bt | Pl | Grt | Bt | Pl |
| SiO ₂ wt% | 38.22 | 51.49 | 50.32 | 37.96 | 50.02 | 51.86 | 38.56 | 51.75 | 47.43 | 38.03 | 36.53 | 61.55 | 37.78 | 35.13 | 59.10 |
| TiO ₂ | 0.01 | 0.24 | 0.01 | 0.01 | 0.47 | 0.01 | 0.01 | 0.01 | 0.01 | 0.01 | 1.90 | 0.01 | 0.01 | 3.05 | 0.13 |
| Al ₂ O ₃ | 21.72 | 1.82 | 30.74 | 21.15 | 3.48 | 29.76 | 21.06 | 1.75 | 31.38 | 21.91 | 17.97 | 23.82 | 21.42 | 18.28 | 25.31 |
| Cr ₂ O ₃ | 0.02 | 0.04 | 0.01 | 0.10 | 0.01 | 0.02 | 0.01 | 0.07 | 0.01 | 0.10 | 0.29 | 0.01 | 0.01 | 0.09 | 0.01 |
| FeO | 26.35 | 10.38 | 0.01 | 24.27 | 8.11 | 0.01 | 25.18 | 21.69 | 0.28 | 30.70 | 12.39 | 0.01 | 33.81 | 17.96 | 0.20 |
| MnO | 0.97 | 0.28 | 0.01 | 0.82 | 0.01 | 0.01 | 0.83 | 0.19 | 0.01 | 0.86 | 0.01 | 0.01 | 1.61 | 0.01 | 0.01 |
| MgO | 3.53 | 11.71 | 0.01 | 6.38 | 12.73 | 0.01 | 6.16 | 21.99 | 0.01 | 5.57 | 15.34 | 0.01 | 3.77 | 9.90 | 0.01 |
| CaO | 10.36 | 23.25 | 13.20 | 6.64 | 22.17 | 12.10 | 6.89 | 0.46 | 15.33 | 3.69 | 0.01 | 5.48 | 2.35 | 0.01 | 7.15 |
| Na ₂ O | 0.01 | 0.39 | 3.99 | 0.01 | 0.58 | 4.42 | 0.01 | 0.01 | 2.70 | 0.02 | 0.24 | 8.96 | 0.01 | 0.16 | 7.57 |
| K ₂ O | 0.01 | 0.01 | 0.01 | 0.01 | 0.01 | 0.13 | 0.01 | 0.01 | 0.01 | 0.07 | 9.19 | 0.01 | 0.18 | 9.77 | 0.13 |
| Sum | 101.20 | 99.61 | 98.31 | 97.35 | 97.59 | 98.33 | 98.72 | 97.93 | 97.17 | 100.96 | 93.87 | 99.87 | 100.95 | 94.36 | 99.62 |

Mineral symbols after Kretz (1983). All Fe is assumed to be in the ferrous state.

PETROGRAPHIC OBSERVATIONS

Four Peaks domain

Metabasites in this area, including both Archean supracrustal rocks and Proterozoic dykes, are characterized by the assemblages Grt – Cpx – Pl – Qtz ± Opx or Hbl – Pl – Qtz ± Grt (Fig. 5a), both of which are interpreted to have developed during D_{n+2} deformation (coeval with the formation of the ASZ; Van Kranendonk *et al.* 1994). In a few samples of the mafic dykes, there is no Hbl associated with the Grt–Cpx subassemblage, but the majority show evidence of Hbl replacing Grt or Cpx (or both), suggesting that there was variable progress of the generalized decompression-hydration reaction $\text{Grt} + \text{Cpx} + \text{H}_2\text{O} = \text{Hbl} + \text{Pl}$ after the main D_{n+2} event. In Hbl-free or Hbl-poor samples, incipient formation of Opx–Pl symplectite at Grt – Cpx interfaces attests to initiation of the generalized anhydrous decompression reaction $\text{Grt} + \text{Cpx} = \text{Opx} + \text{Pl}$. Some of the Proterozoic dykes contain thin veins (0.5 cm) with the subassemblage Grt – Cpx, implying preservation of the prograde products of the generalized dehydration reaction $\text{Hbl} + \text{Pl} = \text{Grt} + \text{Cpx} + \text{H}_2\text{O}$. The presence of calcite (Fig. 5b; Mengel & Rivers 1992) and, locally, scapolite (Van Kranendonk

& Wardle, in press) in these veins suggests that preservation of the Grt – Cpx assemblage may in part have been due to the presence of a CO₂-rich fluid phase.

A similar Proterozoic Grt – Cpx – Pl overprint on the Avayalik dykes and Late Archean (Scott 1995a) Opx – Cpx – Pl granulite-facies assemblages occurs in gneisses in the Seven Islands Bay area farther south (Fig. 1; Wardle *et al.* 1994, Van Kranendonk & Wardle 1997). In that area, grains of orthopyroxene are rimmed by a prograde corona of Cpx – Grt, without the involvement of Hbl. Subsequent decompression is shown by a variably developed rim of Pl on Grt. In the Four Peaks domain, the prograde reactions took place during D_{n+2} transcurrent shearing along the ASZ, when the area was buried obliquely below the Burwell domain. Decompression features, on the other hand, developed as a result of D_{n+3} shearing and exhumation along the eastern KSZ (Van Kranendonk & Wardle 1996, 1997, Van Kranendonk & Mengel 1996).

In summary, there is evidence for a static metamorphic event (D_{n+2}) that led to formation of the assemblage Grt – Cpx, which variably overprinted Archean granulite-facies assemblages. This was followed by decompression or hydration (or both),

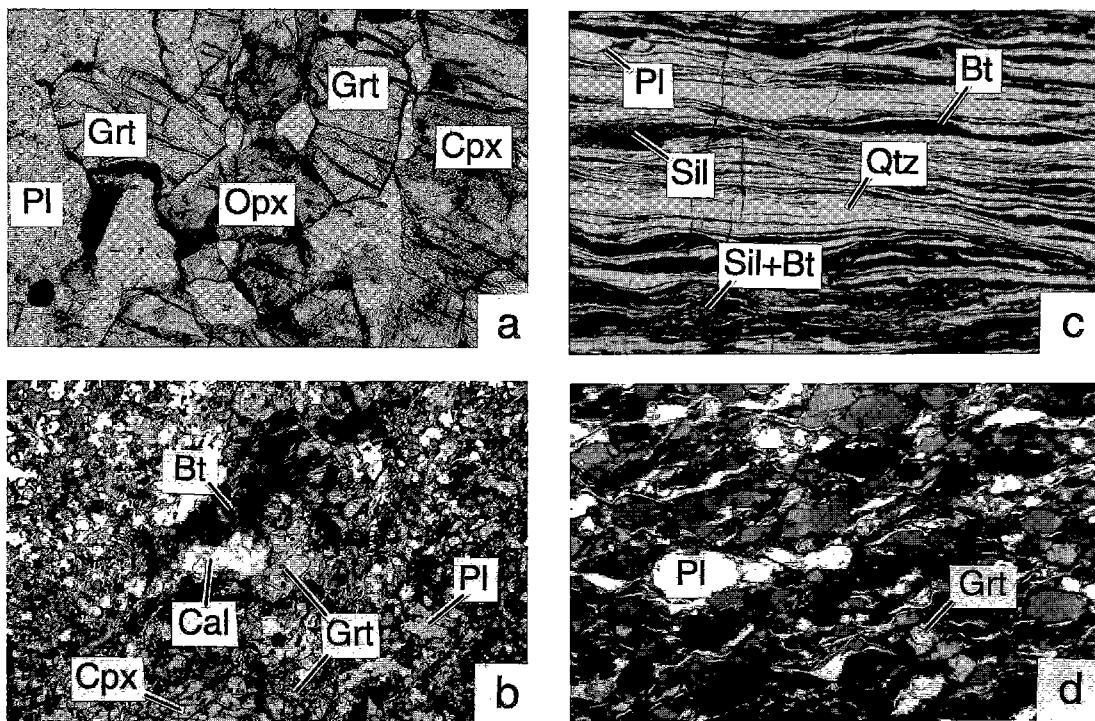


FIG. 5. Selected examples of microstructural and paragenetic features described in the text (all photomicrographs in plane-polarized light; w: width of photomicrograph). (a) Grt-Cpx-Opx-Pl-Qtz assemblage from mafic layer in supracrustal sequence. Sample 25b, w = 3.5 mm. (b) Calcite and biotite in Grt-Cpx vein (lower left to upper right) in an Avayalik dyke. Note small laths of Pl outside vein. Sample 31, w = 3.5 mm. (c) Ribbon mylonite developed in Grt-Bt-Sil-bearing metapelite. Note shear bands. Sample 13d, w = 7 mm. (d) Deformed Avayalik dyke. Hbl and Grt porphyroclasts in Pl-Qtz matrix. Sample 13g, w = 7 mm.

leading to the formation of Opx - Pl and Hbl - Pl assemblages during the D_{n+3} event. Some rocks went directly from Grt - Cpx to Hbl - Pl, whereas others went through an intermediate Opx - Pl stage, the variation presumably being due to the availability of H_2O .

The Komaktorvik shear zone

Rocks from within the Komaktorvik shear zone show a variable intensity of fabric development due to the anastomosing nature of the zones of strain. Highly strained samples are mylonites and ultramylonites (e.g., Fig. 5c), whereas the least-strained rocks are foliated or augen gneisses (Fig. 5d). The highest strains are observed in discontinuous, unlinked, 1-5 km wide strands, which can be traced for up to 30 km along strike (e.g., Van Kranendonk & Wardle 1996).

Metabasic supracrustal rocks typically display the assemblage Grt - Hbl - Pl - Qtz (Fig. 5e). The assemblage Grt - Cpx - Pl - Hbl - Qtz occurs locally and always with petrographic evidence of hornblende replacing clinopyroxene, implying operation of the generalized reaction $Grt + Cpx + H_2O = Hbl + Pl$.

Proterozoic dykes and gabbro are also composed of the assemblage Grt - Hbl - Pl - Qtz \pm Cpx (Fig. 5f), with the amount of garnet being quite variable. In both lithologies, hornblende with typical brown-green pleochroism is locally rimmed by blue-green amphibole (actinolite), and epidote occurs in a few samples. Subareas of thin sections with these features were avoided for thermobarometry.

Pelitic rocks in the Komaktorvik shear zone contain the assemblage Grt - Bt - Sil - Pl - Qtz - Kfs \pm Rt. Sillimanite occurs as both prismatic grains and as late fibrolite on grain boundaries, and grains of garnet

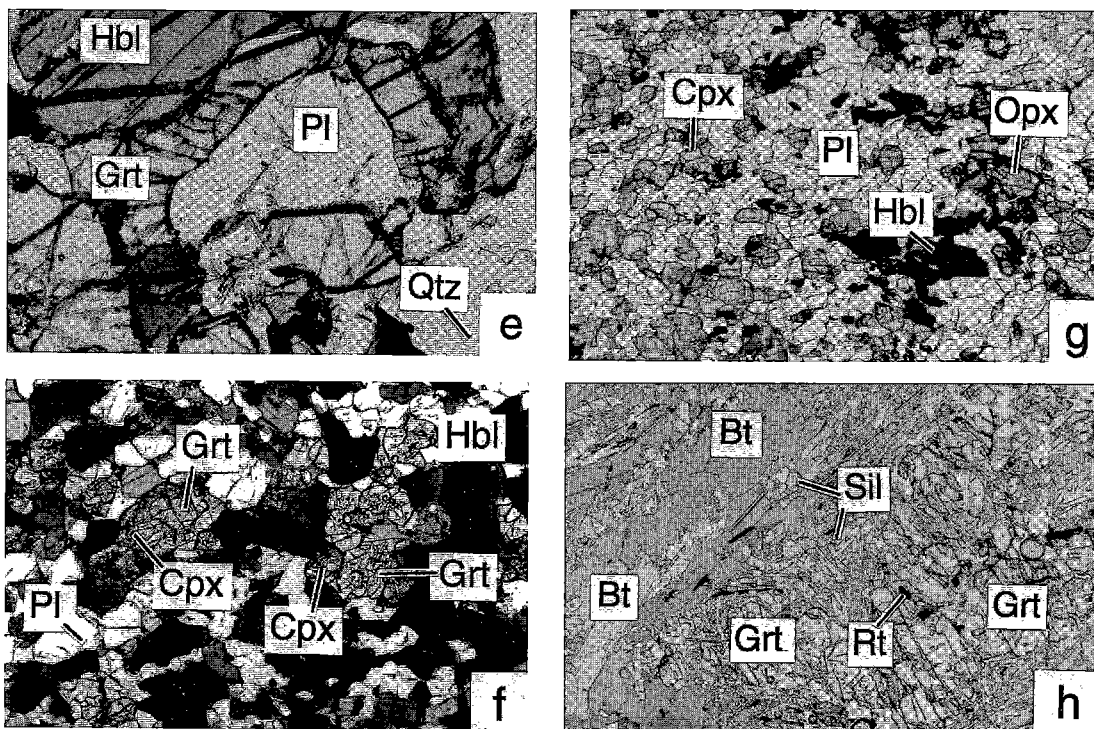


FIG. 5 (continued). (e) Pl partially rimmed by Grt and Hbl. Sample 4a, $w = 1.4$ mm. (f) Grt-Cpx-Hbl-Pl assemblage in recrystallized Avayalik dyke. Sample 147g, $w = 3.5$ mm. (g) Charnockite with the assemblage Opx-Cpx-Hbl-Pl. Sample 178a, $w = 7$ mm. (h) Metapelite with Grt-Bt-Sil-Rt assemblage. Sample 197, $w = 3.5$ mm.

commonly preserve trails of inclusions of sillimanite defining a former folded foliation. The K-feldspar is perthitic microcline. Although not present in our samples, relict kyanite also has been observed, and there is petrographic evidence that it preceded sillimanite (Patey 1994, 1995, Van Kranendonk & Wardle 1996).

The Burwell domain

Both prograde and retrograde transitions are observed in the variably foliated and lineated amphibolite- to granulite-facies intrusive rocks of the Burwell domain (Van Kranendonk & Wardle, in press). Conditions of peak metamorphism are recorded by the assemblage Opx - Hbl - Pl - Qtz \pm (Cpx, Grt) (Fig. 5g). The amount of hornblende is quite variable, with petrographic evidence of hornblende replacing

orthopyroxene and clinopyroxene in many thin sections. Pelitic rocks west of the KSZ contain the assemblage Grt - Bt - Sil - Pl - Qtz - Kfs \pm Rt \pm Ilm (Fig. 5h).

MINERAL COMPOSITIONS

The chemical composition of selected minerals (Tables 2, 3) was determined with an electron microprobe. Operating conditions are given in the Appendix.

Hornblende

The compositional differences among grains of amphibole ("hornblende" in the following) from the study area were found to be minor, regardless of lithology and geographic position. Hence all amphiboles are considered together below. No

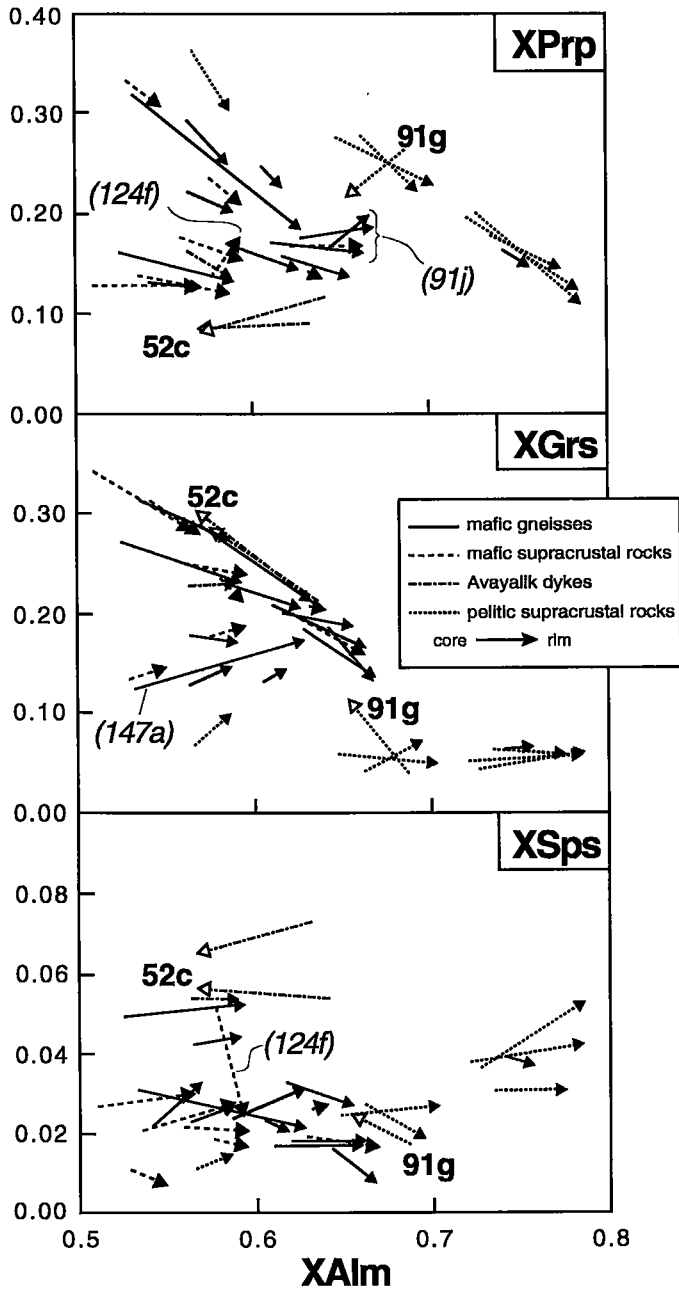


FIG. 6. Patterns of zoning in selected grains of garnet from the main lithological groups. Each arrow points from core to rim compositions. Open arrowheads and bold text pertain to garnet grains showing "prograde zoning" (X_{Alm} decrease toward the rim), whereas filled arrows are used for the remainder, all showing rimward increase in X_{Alm} . Full lines: mafic gneisses, stippled lines: mafic supracrustal rocks, dash-dot lines: Avayalik dykes, dotted lines: pelitic supracrustal rocks. Sample numbers in italics pertain to garnet showing "deviating" patterns of zoning (see text). Note different scale along ordinate in X_{Alm} versus X_{Sps} .

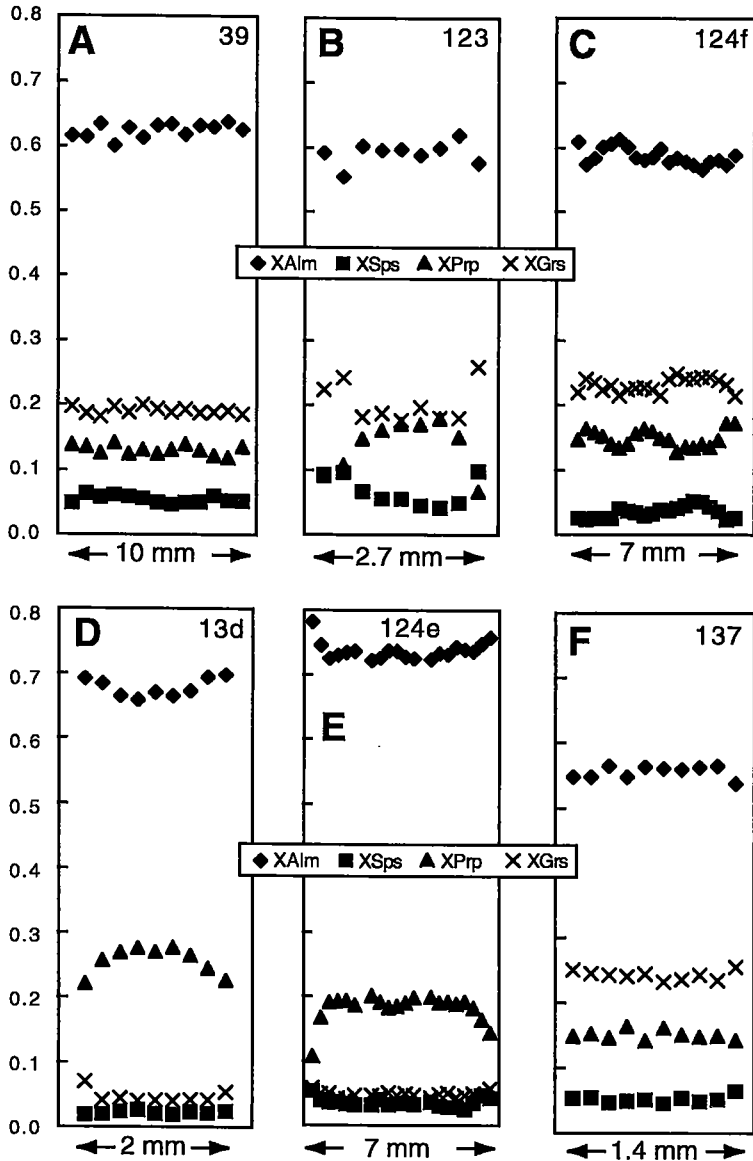


FIG. 7. Compositional profiles in garnet from the western part of the KSZ. (A)–(C): 39, 123 and 124f are mafic supracrustal rocks, (D), (E): 13d and 124e are pelitic supracrustal rocks, (F): 137 is an Avayalik dyke.

compositional zoning was detected in any of the grains analyzed, which range from edenite, through ferro-edenite and pargasite, to ferropargasite for those with $(\text{Na} + \text{K})_{\text{A}} > 0.5$, and from magnesiohornblende to ferrohornblende for those with $(\text{Na} + \text{K})_{\text{A}} < 0.5$ (classification of Leake *et al.* 1997).

Garnet

Garnet occurs in all the rock types investigated. In mafic orthogneisses, the compositional range is $\text{Alm}_{50-65}\text{Prp}_{11-25}\text{Grs}_{13-30}\text{Sps}_{1-6}$, very similar to that in mafic supracrustal gneisses ($\text{Alm}_{51-65}\text{Prp}_{9-33}\text{Grs}_{10-34}\text{Sps}_{0-4}$).

Garnet from the mafic Proterozoic Avayalik dykes have slightly lower Prp ($\text{Alm}_{56-64}\text{Prp}_{7-17}\text{Grs}_{15-30}\text{Sps}_{0-8}$). Garnet from pelitic metasedimentary rocks is more Alm-rich and Grs-poor, in the range $\text{Alm}_{55-78}\text{Prp}_{10-36}\text{Grs}_{3-23}\text{Sps}_{0-4}$ ($\text{Alm}_{55-78}\text{Prp}_{12-36}\text{Grs}_{3-11}\text{Sps}_{0-4}$ if one Ca-rich rock is excluded). Within individual samples, the compositional variation rarely exceeds 5 mol.% of individual end-members, and largely stems from compositional zoning.

Core-to-rim compositional variations in selected grains of garnet from the study area are shown in Figure 6. The majority of the samples conform broadly to the same patterns; however, grains of garnet from pelites stand out with respect to both their overall composition and their patterns of zoning. These grains show a rimward increase of X_{Alm} and X_{Sps} , and decrease of X_{Prp} , X_{Grs} , however, shows very little change, consistent with retrograde cooling (in equilibrium with Sil-Pl-Qtz; Martignole & Nantel 1982). Grains of garnet in mafic supracrustal rocks display a fairly systematic rimward increase of X_{Alm} , decrease of X_{Prp} , whereas X_{Sps} and X_{Grs} trends are less clear. The garnet from mafic gneisses generally shows the same patterns of zoning as those in mafic supracrustal rocks. The patterns of zoning described above are interpreted to be the result of continued re-equilibration after peak conditions of metamorphism.

In contrast, "prograde" growth zoning (*i.e.*, rimward decrease in X_{Alm}) has only been observed in garnet from two samples (open arrows in Fig. 6). Both are from the eastern, highly strained part of the KSZ, and preserve evidence of garnet replacing earlier hydrous minerals. Sample 52c, an Avayalik dyke, shows garnet replacing hornblende, whereas clear Grt in sample 91g, a metapelite, replaces biotite. Similar patterns of zoning have been reported from farther south in the KSZ (20 and 80 km south of the present study-area), and interpreted to reflect prograde growth during D_{n+3} burial of the eastern KSZ (Van Kranendonk & Wardle 1997).

Figure 7 shows typical compositional traverses across grains of garnet from mafic supracrustal rocks (A-C), pelitic supracrustal rocks (D, E) and an Avayalik dyke (F). Only D and E show systematic variations (core-to-rim increase in X_{Alm} and decrease of X_{Prp}), whereas the others show variably "flat" central portions combined with post-peak retrogression and re-equilibration recorded in grain margins (increase of X_{Grs} , X_{Sps}).

Plagioclase

First-order differences in average compositions of plagioclase are largely a function of lithology. For instance, in the metapelites, Avayalik dykes and mafic gneisses, most plagioclase is An_{30-40} , whereas in the Hutton anorthositic suite, it is An_{40-60} , and in some of the metagabbroic rocks, the range may be as large as

An_{22-55} . However, there are also significant differences within single lithological groups that can be related to textural setting. For example, in mafic gneisses, plagioclase that is the product (with orthopyroxene) of the decompression reaction between garnet and clinopyroxene is up to An_{70-80} . Elsewhere, where the composition of both recrystallized matrix plagioclase and fine-grained symplectitic plagioclase are known, the range may be quite large (*e.g.*, An_{30} to An_{64} for sample 107a), but within most samples, the range is less than 10% An. Both normal and reverse zoning occur in plagioclase, but no systematic relationships with respect to mineral assemblages, lithology or geographic position were observed.

Pyroxenes

Orthopyroxene was found in each of the rock types; X_{Mg} ranges from 0.42 to 0.68, with the highest values in mafic and felsic supracrustal rocks. X_{Mg} zoning patterns are generally flat, and Al, which ranges from 0.6 to 2 wt% Al_2O_3 , does not display systematic zoning. *Clinopyroxene* occurs in mafic gneisses, mafic supracrustal rocks and dykes. X_{Mg} ranges from 0.55 to 0.74, with the highest values in mafic supracrustal rocks and anorthositic gneisses (Table 3). The Al content ranges from 1 to 3 wt% Al_2O_3 , and is generally highest in the core of the grains.

Biotite

Biotite occurs in most rock types and samples. It is unzoned, with X_{Mg} ranging from 0.44 to 0.76, and shows the highest values in biotite from pelitic and mafic supracrustal rock types. Among the pelitic supracrustal rocks, X_{Mg} falls into groups of around 0.5 and 0.7, apparently due to bulk-composition controls, as the X_{Mg} of the coexisting garnet shows similar maxima.

RESULTS ON THERMOBAROMETRY

Presentation of P-T data

The activity models and assemblages used for thermobarometry are described in the Appendix. Results are displayed graphically in Figure 8, in which symbols identify both the rock type and the assemblage used. In order to minimize the "non-synchronous closure" problem discussed earlier, Figure 8 only shows peak conditions of P-T inferred for each sample and the range of additional determinations. The full set of P-T data is available from the first author upon request, and from the Depository of Unpublished Data.

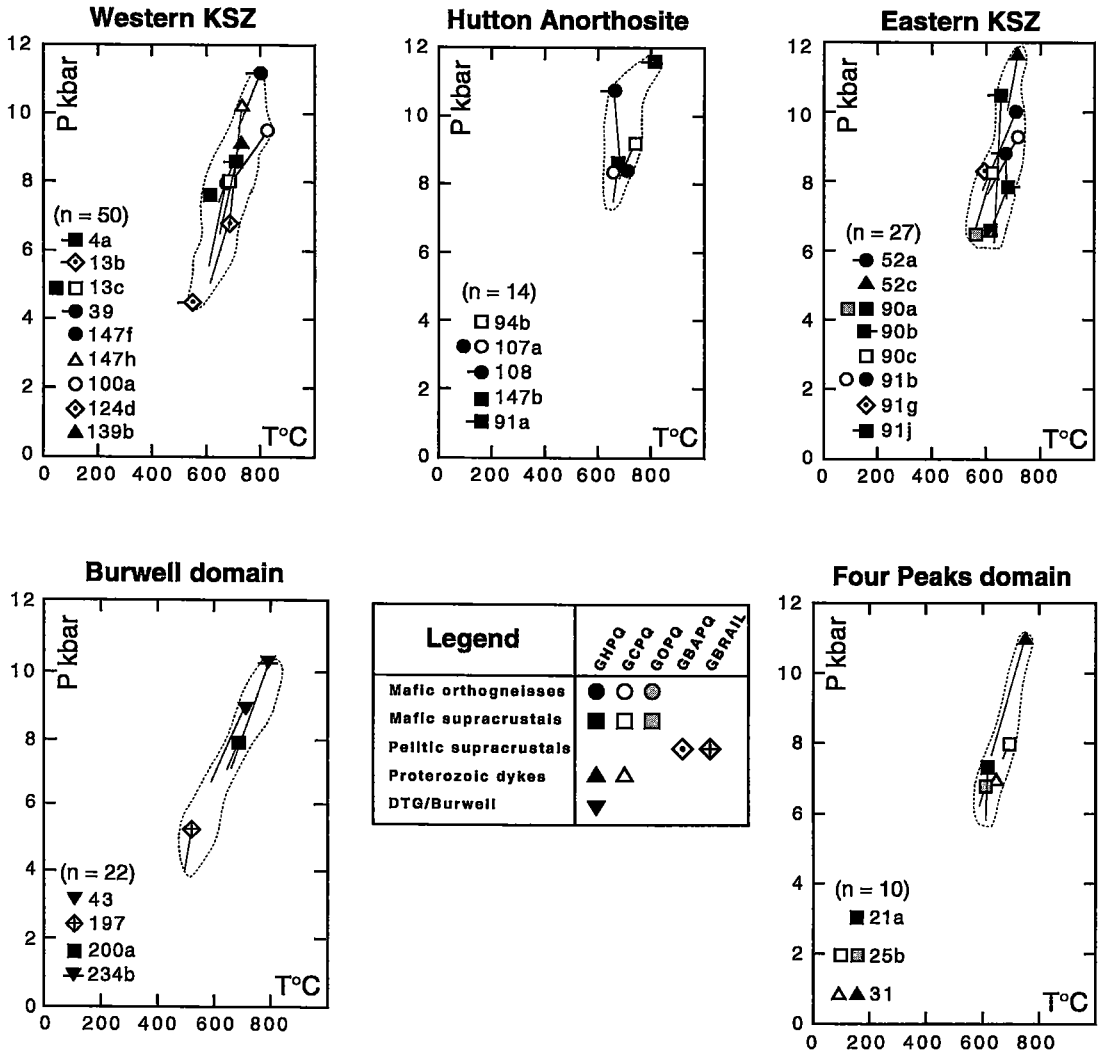


FIG. 8. P-T data from the Four Peaks domain, Komaktorvik shear zone [eastern, central (= Hutton anorthositic suite) and western part] and Burwell domain. For simplicity, only peak determinations for each sample are shown, and the range is indicated by a line. Stippled lines enclose all determinations (n). Small, horizontal tics are used to distinguish samples with similar symbols. In the legend, symbol-fill is linked to type of mineral assemblage used for thermobarometry (open, filled, gray, dot, cross), whereas symbol shape is keyed to lithological types (circle, square, diamond, triangle). "DTG/Burwell" comprises rocks of the DTG and Killinek charnockitic suites in the Burwell domain. For geothermobarometric assemblages, the abbreviations are: G Garnet, H Hornblende, C Clinopyroxene, O Orthopyroxene, B Biotite, A Al-Silicate, R Rutile, IL Ilmenite, P Plagioclase, and Q Quartz. See Appendix for details about the thermobarometric methods employed.

P-T results from the Four Peaks domain (east of the KSZ)

P-T data for all rock types from the Four Peaks domain, where overprinted by the static Paleoproterozoic metamorphism, form a linear array from ca. 11 kbar – 750°C to ca. 6 kbar – 600°C (Fig. 8). The

Avayalik dyke (sample 31, Table 3) yields the highest P-T estimates, with P-T_{GHPQ} being higher than the single P-T_{GCPQ} (note that the acronyms are defined in the caption to Fig. 8). Data from mafic supracrustal rocks form a more restricted cluster at the lower end of the array, in the range 6–8 kbars – 600–700°C. For these estimates, it is noteworthy that values of P_{GORQ} are

lower than values of P_{GCPQ} , in accord with petrographic observations of the generalized decompression reaction $\text{Grt} + \text{Cpx} = \text{Opx} + \text{Pl}$ (where $P\text{-}T_{\text{GCPQ}}$ was determined in textural settings with no evidence for $\text{Opx}\text{-Pl}$ formation from $\text{Grt}\text{-Cpx}$).

P-T results from the KSZ

Data from the KSZ were subdivided into three groups in order to test for systematic differences with respect to location in the shear zone. For each group, the samples form a subconcordant linear array (Fig. 8).

East of the Hutton anorthositic suite (Fig. 2, "Eastern KSZ" in Fig. 8), the highest pressures come from the Avayalik dykes (11.7 kbar – 720°C with GHPQ, Table 3), whereas the lower end of the array (ca. 6 kbar) is recorded in mafic supracrustal rocks. The center of the array is well defined, and includes a core-to-rim variation in the GCPQ assemblage from 8.2 kbar – 620°C to 6.5 kbar – 540°C (sample 90c, Fig. 8). For individual samples, $P\text{-}T_{\text{GHPQ}}$ is generally similar to $P\text{-}T_{\text{GCPQ}}$, but may be higher by up to 2 kbar.

Data from the *Hutton anorthositic suite* (Fig. 8) come from gneissic mafic layers within the anorthosite, including a $\text{Grt}\text{-Hbl}\text{-Pl}\text{-Qtz}$ porphyroclastic mylonitic gneiss along the eastern margin (11.6 kbar – 815°C with GHPQ, Table 3). The remainder of samples from this unit yields a tight array from 9.5 to 7 kbar at ca. 700°C (GHPQ and GCPQ).

Samples from the *KSZ west of the Hutton anorthositic suite* ("Western KSZ" in Fig. 8) yield a similar pattern. High pressures are recorded in the Avayalik dykes (Table 3), and the lowest $P\text{-}T$ results come from pelitic supracrustal rocks, with all data points defining a steep $P\text{-}T$ array. Values of $P\text{-}T_{\text{GHPQ}}$ are equal to or slightly higher than values of $P\text{-}T_{\text{GCPQ}}$, whereas values of $P\text{-}T_{\text{GBAPQ}}$ from pelitic lithologies record lower $P\text{-}T$ conditions, presumably established during later stages of re-equilibration.

$P\text{-}T$ data from the three zones across the KSZ show the same peak $P\text{-}T$ conditions, and the arrays have the same overall orientation (Fig. 8). The degree to which lower-grade conditions are recorded varies according to rock types (metapelites in the Western KSZ record the lowest-grade conditions), but it is also inferred that heterogeneous, domainal re-equilibration is responsible for some of the recorded variation (see Discussion).

P-T results from the Burwell domain (west of the KSZ)

Samples from this area comprise various rock types belonging to the DTG and Killinek charnockitic suites as well as to adjacent pelitic supracrustal rocks. The $P\text{-}T$ data (Fig. 8) define an extended array from ca. 10 kbar – 780°C (mafic granulites from the DTG suite, Table 3) down to ca. 4 kbar – 500°C (pelitic supracrustal rocks).

P-T paths

The $P\text{-}T$ determinations come from a transect across the full width of the KSZ and well into the adjacent unshaped wallrock domains. In any one domain, $P\text{-}T$ arrays defined by each of the four rock types taken individually are parallel to the composite array defined by the whole population. Arrays consisting only of the highest $P\text{-}T$ determinations from each sample (Fig. 8) also are parallel to the composite arrays. Furthermore, where reliable $P\text{-}T$ determinations could be obtained from both core and rim of coexisting minerals, $P\text{-}T$ vectors are again parallel to the overall $P\text{-}T$ array. These observations, together with the fact that the $P\text{-}T$ arrays have significantly steeper slopes than isopleths of the barometric equilibria, support the suggestion that individual samples record different parts of the $P\text{-}T$ path.

The results indicate that the degree of resetting of the geothermometers and geobarometers during cooling was a function of rock type. Comparisons of $P\text{-}T$ determinations in the Avayalik dykes, mafic orthogneisses and mafic supracrustal rocks show that the highest $P\text{-}T$ conditions were most commonly preserved in the Avayalik dykes, indicating that this group of rocks was the most resistant to resetting during cooling, followed by the mafic orthogneisses and the mafic supracrustal rocks, respectively.

Comparisons among the $P\text{-}T$ arrays for the three domains indicate negligible differences, taking into account the errors inherent in geothermobarometry ($\pm 50^\circ\text{C}$, ± 1 kbar). This result is compatible with the predominantly transcurent nature of the KSZ and suggests that the late mylonites with down-dip stretching lineations were not the loci of major displacements.

The degree to which peak $P\text{-}T$ conditions are preserved is uncertain. Considering the sample population as a whole, $P\text{-}T_{\text{GHPQ}}$ is generally similar to or greater than $P\text{-}T_{\text{GCPQ}}$, as noted above, but this could be interpreted in several ways: (1) variable access of H_2O -rich fluid before, during and after attainment of peak $P\text{-}T$, (2) incorrect calibration of the geothermobarometers (*i.e.*, overestimation of $P\text{-}T$ with GHPQ or underestimation of $P\text{-}T$ with GCPQ, or both), or (3) an effect of relative rates of diffusion during retrogression, indicating that diffusion is slower in hornblende than in clinopyroxene. Several samples containing both hornblende and clinopyroxene illustrate that $P\text{-}T_{\text{GHPQ}}$ is generally similar to $P\text{-}T_{\text{GCPQ}}$; this finding rules out (2) as the main source of the discrepancy, but we are unable to distinguish between (1) and (3) with the present data-set.

The near-ITD signatures displayed by the $P\text{-}T$ arrays in each domain, together with the widespread preservation of high-pressure assemblages (and

local preservation of prograde features), suggest that exhumation of all three domains was sufficiently rapid that higher-grade assemblages did not thoroughly re-equilibrate. The degree to which samples have recorded retrograde conditions is inferred to be a result of variable reaction-progress during cooling, which itself is a complex function of the mineral assemblage, strain and the availability and composition of fluids during retrogression.

Relationship between deformation and metamorphism

As noted earlier, samples from the KSZ are moderately to strongly lineated, with hornblende in mafic rocks defining the gently plunging D_{n+3} stretching lineation. Combined with the P–T data presented above, this observation suggests that both the D_{n+3} shearing and the retrograde reactions that led to the formation of hornblende in the mafic rocks took place over a range of P–T conditions, including at or near the peak of metamorphism.

The concordance of estimates of the maximum P–T and the slopes of P–T paths from across the entire transect can be explained by two end-member models: (1) the KSZ and neighboring domains went through the P–T–t history synchronously, and the late mylonites did not accommodate much vertical displacement after closure of the thermobarometric systems; (2) the KSZ and neighboring domains were exhumed at different times, but, as shown by the geometry of the P–T paths, the cumulative rates and amounts of uplift were broadly the same in all domains. Considering only the Burwell and Four Peaks domains initially, the U–Pb data superficially appear to support the latter model, *i.e.*, the range in ages of metamorphism as defined by U–Pb zircon data is 1875–1816 Ma in the Burwell domain compared to 1834–1719 Ma in the Four Peaks domain (Fig. 4). However, the wide spread of U–Pb zircon ages (59 M.y. in Burwell domain and 115 M.y. in Four Peaks domain) in such narrow domains suggests that many of the ages do not date the closure temperatures, but probably represent metamorphic growth of zircon below its closure temperature due to other factors, such as dynamic recrystallization during shearing or the influx of metamorphic fluids. In support of this hypothesis, we note that the highest determinations of metamorphic temperature in all three domains are in the range 800–750°C (Fig. 8), below the closure temperature of Pb diffusion in zircon (>800°C: Heaman & Parrish 1991). The role of dynamic recrystallization in particular as a factor facilitating growth of zircon below its closure temperature is supported by the observation that the oldest age in the Four Peaks domain comes from a statically recrystallized Avayalik dyke, in which the effects of dynamic recrystallization might be expected to be

minimal. If post-peak growth of zircon due to dynamic recrystallization was widespread, the age of peak metamorphism cannot be unambiguously interpreted from the data, as even the oldest determined age may represent post-peak growth of zircon.

These arguments can be extended to the interpretation of the U–Pb zircon data for the age of metamorphism in KSZ. In this case, the measured range in ages is 1795–1750 Ma, superficially implying that metamorphism was initiated >30 M.y. later than in the adjacent Burwell and Four Peaks domains. However, our preferred interpretation is that the penetrative D_{n+3} shearing in the KSZ resulted in the almost universal recrystallization of D_{n+2} metamorphic zircon, with the result that evidence for metamorphic growth during D_{n+2} in the KSZ has so far eluded detection. In support of this hypothesis, Figure 4 shows that there is a 30 M.y. overlap of zircon and titanite ages (between 1775 and 1745 Ma), during which both zircon and titanite closed to Pb diffusion in different samples, a pattern that is incompatible with a simple model based on closure temperature.

Comparison of the data for the Burwell domain and the KSZ indicates that at 1800–1780 Ma, rocks in the KSZ were at 11.7 kbar – 800°C and undergoing strain in a transcurrent shear-zone, whereas those in the Burwell domain had already experienced their peak of metamorphism and were undergoing exhumation and isothermal decompression. This pattern is compatible with an overall younging of the exhumation process from the hinterland toward the foreland of the Torngat Orogen.

In summary, the Paleoproterozoic granulite-facies event affecting the Archean granulite-facies rocks in the western margin of the Four Peaks domain was coeval with D_{n+2} , on the basis of interpretations of U–Pb ages in the metamorphosed Avayalik dykes (1843 Ma in the Burwell domain, 1834 Ma in the Four Peaks domain: Van Kranendonk & Wardle 1996, 1997; Fig. 4). D_{n+2} involved oblique tectonic burial of the western margin of the Four Peaks domain beneath the Burwell domain synchronously with the formation of the Abloviak shear zone in the central Torngat Orogen at 1845–1822 Ma (Bertrand *et al.* 1933, Scott & Machado 1995, Van Kranendonk & Wardle 1996, 1997). Penetrative sinistral transcurrent shearing in the KSZ occurred *ca.* 1800–1780 Ma during D_{n+3} , in association with east–west contraction and folding of the thickened crust. Zircon is inferred to have dynamically recrystallized throughout the KSZ at this time. D_{n+3} shearing in the KSZ was coeval with the early stages of exhumation and unroofing in adjacent Burwell and Four Peak domains. Later deformation in the KSZ and Four Peaks domain, recorded by the narrow, D_{n+4} lower-amphibolite-facies mylonites with down-dip stretching lineations and by the intrusion of syntectonic granitic pegmatites and sheets of granite, took place

episodically between 1791 and 1710 Ma (Scott & Machado 1995) and was associated with the later stages of unroofing and exhumation (Van Kranendonk & Wardle 1996, 1997).

CONCLUSIONS

In conclusion, the study of the metamorphic evolution in the northern Torngat Orogen, focused on the Komaktorvik shear zone and its adjacent blocks, has shown that:

- 1) Gneisses and supracrustal rocks of the Four Peaks domain east of the KSZ experienced a static Paleoproterozoic metamorphic overprint during D_{n+2} as a result of oblique burial beneath the Burwell domain at ca. 1845–1822 Ma. This thermal event is best monitored by the Avayalik dykes, which record peak conditions of ca. 11 kbar – 750°C.
- 2) Peak conditions of metamorphism determined within the KSZ were ca. 11.7 kbar – 800°C, and were reached during D_{n+3} at ca. 1800–1780 Ma.
- 3) Peak conditions of metamorphism in the Burwell domain west of the KSZ were ca. 10 kbar – 790°C, and were reached during D_{n+2} at ca. 1840–1835 Ma.
- 4) In each of the three domains, post-peak retrogression and re-equilibration are shown by decompression or hydration reactions (or both).
- 5) The P–T arrays in all three domains are similar and record isothermal decompression (ITD).
- 6) In each of the three domains, P–T arrays from individual samples and rock types overlap with the composite array for the whole population.
- 7) The maximum P–T recorded by the assemblages is a function of both the rock type and the assemblage used for geothermobarometry. Highest values of pressure and temperature were derived from the Avayalik dykes, with the mafic orthogneisses, mafic and pelitic supracrustal rocks recording progressively lower values.
- 8) Although the P–T arrays for each domain are similar, geochronological data suggest that zircon in the KSZ crystallized some 40 M.y. after zircon in adjacent domains. Furthermore, within each domain, determinations of the age of metamorphism by a single method (e.g., U–Pb zircon) show a span of >50 M.y., and U–Pb zircon and titanite ages overlap. These data are interpreted to indicate new growth of zircon and titanite below their closure temperature as a result of dynamic recrystallization during shearing or the ingress of metamorphic fluids (or both).
- 9) Transcurrent movement on the KSZ was coeval with the early stages of exhumation in the adjacent domains.
- 10) This study has demonstrated the importance of (1) analyzing both peak and post-peak mineral assemblages in a range of rock types to obtain the P–T path, and (2) linking structural and metamorphic observations with geochronological data from well-constrained, carefully chosen samples.

ACKNOWLEDGEMENTS

We are grateful to the leaders of the Torngat mapping project and their associated organizations (Dick Wardle, Newfoundland Department of Mines and Energy, and Martin Van Kranendonk, then at the Geological Survey of Canada) for help and support in the field. FM thanks the Danish Natural Sciences Research Council for fellowships, and TR acknowledges funding from NSERC and LITHOPROBE. FM thanks Jørn Rønso and John Fløng for maintaining an excellent electron-microprobe facility in Copenhagen. Dick Wardle and Dave Scott commented constructively on earlier versions of the manuscript. Guest Editor Rob Berman and reviewers Ed Ghent and Martin Van Kranendonk provided exhaustive, yet thorough and constructive reviews.

REFERENCES

- BERMAN, R.G. (1988): Internally-consistent thermodynamic data for minerals in the system $\text{Na}_2\text{O}-\text{K}_2\text{O}-\text{CaO}-\text{MgO}-\text{FeO}-\text{Fe}_2\text{O}_3-\text{Al}_2\text{O}_3-\text{SiO}_2-\text{TiO}_2-\text{H}_2\text{O}-\text{CO}_2$. *J. Petrol.* **29**, 445-522.
- _____ (1990): Mixing properties of Ca–Mg–Fe–Mn garnets. *Am. Mineral.* **75**, 328-344.
- _____ (1991): Thermobarometry using multi-equilibrium calculations: a new technique, with petrological applications. *Can. Mineral.* **29**, 833-855.
- BERTRAND, J.-M., RODDICK, J.C., VAN KRANENDONK, M.J. & ERMANOVICS, I. (1993): U–Pb geochronology of deformation and metamorphism across a central transect of the Early Proterozoic Torngat Orogen, North River map area, Labrador. *Can. J. Earth Sci.* **30**, 1470-1489.
- CAMPBELL, L.M., BRIDGWATER, D. & FARMER, L. (1995): A comparison of Proterozoic crustal formation along the Torngat – Nagssugtoqidian – Lapland collision belts: preliminary constraints from Nd and Pb isotopic studies in northern Labrador. In Eastern Canadian Onshore-Offshore Transect (ECSOOT), Transect Meeting (November 28-29, 1994; R.J. Wardle & J. Hall, compilers). *LITHOPROBE Rep.* **45**, 22-36.
- CONNELLY, J. & MENGEL, F. (1995): Preliminary U–Pb data from Archean gneisses in a transect across the Komaktorvik shear zone, northern Torngat Orogen. In Eastern Canadian Onshore-Offshore Transect (ECSOOT), Transect Meeting (November 28-29, 1994; R.J. Wardle & J. Hall, compilers). *LITHOPROBE Rep.* **45**, 72-82.
- _____ & _____ (1996): The Archean backdrop to Paleoproterozoic tectonism in the Nagssugtoqidian and Torngat Orogens: new constraints from U–Pb geochronology. In Eastern Canadian Onshore-Offshore Transect (ECSOOT), Transect Meeting (March 14-15, 1996; R.J. Wardle & J. Hall, compilers). *LITHOPROBE Rep.* **57**, 15-22.

- DEWEY, J.F. (1988): Extensional collapse of orogens. *Tectonics* **7**, 1123-1140.
- ENGLAND, P.C. & RICHARDSON, S.W. (1977): The influence of erosion upon the mineral facies of rocks from different metamorphic environments. *J. Geol. Soc. London* **134**, 201-213.
- _____ & THOMPSON, A.B. (1984): Pressure-temperature-time paths of regional metamorphism. I. Heat transfer during the evolution of regions of thickened continental crust. *J. Petrol.* **25**, 894-928.
- ERMANOVICS, I.E. & VAN KRANENDONK, M.J. (1990): The Torngat Orogen in the North River - Nutak transect area of Nain and Churchill provinces. *Geosci. Can.* **17**, 279-283.
- FROST, B.R. & CHACKO, T. (1989): The granulite uncertainty principle: limitations on thermometry in granulites. *J. Geol.* **97**, 435-450.
- _____ & TRACY, R.J. (1991): P-T paths from zoned garnets: some minimum criteria. *Am. J. Sci.* **291**, 917-939.
- FUHRMAN, M.L. & LINDSLEY, D.H. (1988): Ternary-feldspar modelling and thermometry. *Am. Mineral.* **73**, 201-215.
- HARLEY, S.L. (1989): The origin of granulites: a metamorphic perspective. *Geol. Mag.* **126**, 215-247.
- HEAMAN, L. & PARRISH, R. (1991): U-Pb geochronology of accessory minerals. In Applications of Radiogenic Isotope Systems to Problems in Geology (L. Heaman & J.N. Ludden, eds.). *Mineral. Assoc. Can., Short Course Handbook* **19**, 59-102.
- HODGES, K.V. & ROYDEN, L. (1984): Geologic thermobarometry of retrograded metamorphic rocks: an indication of the uplift trajectory of a portion of the northern Scandinavian Caledonides. *J. Geophys. Res.* **89**, 7077-7090.
- HOFFMAN, P.F. (1989): Precambrian geology and tectonic history of North America. In *The Geology of North America - An Overview* (A.W. Bally & A.R. Palmer, eds.). The Geological Society of America, Boulder, Colorado (A: 447-512).
- JACKSON, G.D. & TAYLOR, F.C. (1972): Correlation of major Apebian rock units in the northeastern Canadian Shield. *Can. J. Earth Sci.* **9**, 1659-1669.
- KNIGHT, I. & MORGAN, W.C. (1981): The Apebian Ramah Group, northern Labrador. In *Proterozoic Basins of Canada* (F.H. Campbell, ed.). *Geol. Surv. Can., Pap.* **81-10**, 313-330.
- KORSTGÅRD, J.A., RYAN, A.B. & WARDLE, R.J. (1987): The boundary between Proterozoic and Archean blocks in central West Greenland and northern Labrador. In *Evolution of the Lewisian and Comparable Precambrian High Grade Terrains* (R.G. Park & J. Tarney, eds.). *Geol. Soc., Spec. Publ.* **27**, 247-259.
- KRETZ, R. (1983): Symbols for rock-forming minerals. *Am. Mineral.* **68**, 277-279.
- LEAKE, B.E. and 21 others (1997): Nomenclature of amphiboles: report of the subcommittee on amphiboles of the International Mineralogical Association, Commission on New Minerals and Mineral Names. *Can. Mineral.* **35**, 219-246.
- MÄDER, U.K., PERCIVAL, J.A. & BERMAN, R.G. (1994): Thermobarometry of garnet - clinopyroxene - hornblende granulites from the Kapuskasing structural zone. *Can. J. Earth. Sci.* **31**, 1134-1145.
- MARTIGNOLE, J. & NANTEL, S. (1982): Geothermobarometry of cordierite-bearing metapelites near the Morin anorthosite complex, Grenville Province, Quebec. *Can. Mineral.* **20**, 307-318.
- McMULLIN, D.W., BERMAN, R.G. & GREENWOOD, H.J. (1991): Calibration of the SGAM thermobarometer for pelitic rocks using data from phase-equilibrium experiments and natural assemblages. *Can. Mineral.* **29**, 889-908.
- MENGEL, F. (1988): *Thermotectonic Evolution of the Proterozoic-Archaean Boundary in the Saglek Area, Northern Labrador*. Ph.D. thesis, Memorial University of Newfoundland, St. John's, Newfoundland.
- _____ & RIVERS, T. (1990): The synmetamorphic P-T-t path of granulite facies gneisses from Torngat orogen, and its bearing on their tectonic history. *Geosci. Can.* **17**, 288-293.
- _____ & _____ (1991): Decompression reactions and P-T-t paths from individual samples in high grade rocks, northern Labrador: implications for Early Proterozoic tectonic evolution. *J. Petrol.* **32**, 139-167.
- _____ & _____ (1993): 3-Dimensional architecture and thermal structure of a deep crustal-scale transcurrent shear zone. Report 2: Preliminary results from the Komaktorvik shear zone. In *Eastern Canadian Onshore-Offshore Transect (ECSOOT), Transect Meeting* (December 4-5, 1992; R.J. Wardle & J. Hall, compilers). *LITHOPROBE Rep.* **32**, 64-73.
- _____ & _____ (1994): 3-D architecture and thermal structure of a crustal-scale transcurrent shear zone. Report 4: P-T results from the northern Torngat transect. In *Eastern Canadian Onshore-Offshore Transect (ECSOOT), Transect Meeting* (December 10-11, 1993; R.J. Wardle & J. Hall, compilers). *LITHOPROBE Rep.* **36**, 163-170.
- _____, _____ & CONNELLY, J. (1996): Metamorphic signatures in deep crustal shear zones: Abloviak and Komaktorviok shear zones in the Paleoproterozoic Torngat Orogen, northern Labrador. *Geol. Assoc. Can. - Mineral. Assoc. Can., Program Abstr.* **21**, A-65.
- _____, _____ & REYNOLDS, P. (1991): Lithotectonic elements and tectonic evolution of Torngat orogen, Saglek Fiord, northern Labrador. *Can. J. Earth Sci.* **28**, 1407-1423.

- MORGAN, W.C. & TAYLOR, F.C. (1972): Granulite facies metamorphosed basic dykes of the Torngat Mountains, Labrador. *Mineral. Mag.* **38**, 666-669.
- PATEY, B.P. (1994): The metamorphic history of the Proterozoic Komaktorvik Shear Zone: preliminary results. In Eastern Canadian Onshore-Offshore Transect (ECSOOT), Transect Meeting (December 10-11, 1993; R.J. Wardle & J. Hall, compilers). *LITHOPROBE Rep.* **36**, 185-187.
- _____ (1995): Metamorphic history of the Proterozoic Komaktorvik Shear Zone: preliminary thermobarometric results. In Eastern Canadian Onshore-Offshore Transect (ECSOOT), Transect Meeting (November 28-29, 1994; R.J. Wardle & J. Hall, compilers). *LITHOPROBE Rep.* **45**, 200-205.
- PATTISON, D. & BÉGIN, N.J. (1994): Zoning patterns in orthopyroxene and garnet in granulites: implications for geothermometry. *J. Metamorphic Geol.* **12**, 411-428.
- PEACOCK, S.M. (1992): Thermal modeling of metamorphic pressure-temperature-time paths. In *Metamorphic Pressure - Temperature - Time Paths* (F.S. Spear & S.M. Peacock, eds.). *Am. Geophys. Union, Short Course in Geology*, 57-102.
- RIVERS, T., MENGEL, F., SCOTT, D.J., CAMPBELL, L.M. & GOULET, N. (1996): Torngat Orogen - a Paleoproterozoic example of a doubly vergent compressional orogen. In *Precambrian Crustal Evolution in the North Atlantic Regions* (T.S. Brewer, ed.). *Geol. Soc., Spec. Publ.* **112**, 117-136.
- RYAN, B. (1990): Basement-cover relationships and metamorphic patterns in the foreland of the Torngat Orogen in the Saglek-Hebron area, Labrador. *Geosci. Can.* **17**, 276-279.
- _____ (1996): Commentary on the location of the Nain-Churchill boundary in the Nain area. *Newfoundland Dep. Natural Resources, Geol. Surv., Rep.* **96-1**, 109-129.
- SCOTT, D.J. (1995a): U-Pb geochronology of a Paleoproterozoic continental magmatic arc on the western margin of the Archean Nain craton, northern Labrador, Canada. *Can. J. Earth Sci.* **32**, 1870-1882.
- _____ (1995b): U-Pb geochronology of the Nain craton on the eastern margin of the Torngat Orogen, Labrador. *Can. J. Earth Sci.* **32**, 1859-1869.
- _____ & CAMPBELL, L.M. (1993): Evolution of the Paleoproterozoic Torngat Orogen, Labrador, Canada: recent advances using U-Pb geochronology and Nd isotope systematics. *Geol. Soc. Am., Abstr. Program* **25**, A-237.
- _____ & MACHADO, N. (1995): U-Pb geochronology of the northern Torngat Orogen, Labrador, Canada: a record of Paleoproterozoic magmatism and deformation. *Precambrian Res.* **70**, 169-190.
- SILVERSTONE, J. & CHAMBERLAIN, C.P. (1990): Apparent isobaric cooling paths from granulites: two counterexamples from British Columbia and New Hampshire. *Geology* **18**, 307-310.
- SPEAR, F.S. (1992): Petrologic determination of metamorphic pressure - temperature - time paths. In *Metamorphic Pressure - Temperature - Time Paths* (F.S. Spear & S.M. Peacock, eds.). *Am. Geophys. Union, Short Course in Geology*, 1-55.
- _____ (1994): *Metamorphic Phase Equilibria and Pressure - Temperature - Time Paths*. Mineral. Soc. Am., Monogr. 1.
- _____ & FLORENCE, F.P. (1992): Thermobarometry in granulites: pitfalls and new approaches. *Precambrian Res.* **55**, 209-241.
- _____, KOHN, M.J., FLORENCE, F. & MENARD, T. (1990): A model for garnet and plagioclase growth in pelitic schists: implications for thermobarometry and P-T path determinations. *J. Metamorphic Geol.* **8**, 683-696.
- _____, SILVERSTONE, J., HICKMOTT, D., CROWLEY, P. & HODGES, K.V. (1984): P-T paths from garnet zoning: a new technique for deciphering tectonic processes in crystalline terranes. *Geology* **12**, 87-90.
- TAYLOR, F.C. (1979): Reconnaissance geology of a part of the Precambrian shield, northeastern Quebec, northern Labrador, and Northwest Territories. *Geol. Surv. Can., Mem.* **393**.
- THOMPSON, A.B. & ENGLAND, P.C. (1984): Pressure - temperature - time paths of regional metamorphism. II. Their inference and interpretation using mineral assemblages in metamorphic rocks. *J. Petrol.* **25**, 929-955.
- VAN KRANENDONK, M.J. (1990): Structural history and geotectonic evolution of the eastern Torngat Orogen in the North River map area, Labrador. *Geol. Surv. Can., Pap.* **90-1C**, 81-96.
- _____ (1992): *Geological Evolution of the Archean Nain Province and the Early Proterozoic Orogen as Seen along a Transect in the North River - Nutak Map Area, Northern Labrador, Canada*. Ph.D. thesis, Queen's University, Kingston, Ontario.
- _____ (1996): Tectonic evolution of the Paleoproterozoic Torngat Orogen: evidence from pressure - temperature - time - deformation paths in the North River map area, Labrador. *Tectonics* **15**, 843-869.
- _____ & ERMANOVICS, I.E. (1990): Structural evolution of the Hudsonian Torngat orogen in the North River map area, Labrador: evidence for east-west transpressive collision of Nain and Rae continental blocks. *Geosci. Can.* **17**, 283-288.
- _____, GODIN, L., MENGEL, F.C., SCOTT, D.J., WARDLE, R.J., CAMPBELL, L.M. & BRIDGWATER, D. (1993a):

Geology and structural development of the Archaean to Paleoproterozoic Burwell domain, northern Torngat Orogen, Labrador and Quebec. *Geol. Surv. Can., Pap.* **93-1C**, 329-340.

_____ & MENGEL, F. (1996): Metamorphism in the Paleoproterozoic Torngat orogen, northern Labrador: structural and geochronological constraints. *Geol. Assoc. Can. - Mineral. Assoc. Can., Program Abstr.* **21**, A-98.

_____, ST-ONGE, M.R. & HENDERSON, J.R. (1993b): Paleoproterozoic tectonic assembly of Northeast Laurentia through multiple indentations. *Precambrian Res.* **63**, 325-347.

_____ & SCOTT, D.J. (1992): Preliminary report on the geology and structural evolution of the Komaktorvik Zone of the Early Proterozoic Torngat Orogen, Eclipse Harbour area, northern Labrador. *Geol. Surv. Can., Pap.* **92-1C**, 59-68.

_____ & WARDLE, R.J. (1994): Geological synthesis and musings on possible subduction-accretion models in the formation of the northern Torngat Orogen. In Eastern Canadian Onshore-Offshore Transect (ECSOOT), Transect Meeting (December 10-11, 1993; R.J. Wardle & J. Hall, compilers). *LITHOPROBE Rep.* **36**, 62-80.

_____ & _____ (1996): Burwell domain of the Paleoproterozoic Torngat Orogen: tilted cross-section of a magmatic arc caught between a rock and a hard place. In Precambrian Crustal Evolution in the North Atlantic Region (T.S. Brewer, ed.). *Geol. Soc., Spec. Publ.* **112**, 91-116.

_____ & _____ (1997): Crustal-scale flexural slip folding during late tectonic amplification of an orogenic boundary perturbation in the Paleoproterozoic Torngat Orogen, NE Canada. *Can. J. Earth. Sci.* **34** (in press).

_____, _____, MENGEL, F.C., CAMPBELL, L.M. & REID, L. (1994): New results and summary of the Archaean and Paleoproterozoic geology of the Burwell domain, northern Torngat Orogen, Labrador, Quebec and

Northwest Territories. *Geol. Surv. Can., Current Res.* **1994-C**, 321-332.

_____, _____, _____, RYAN, B. & RIVERS, T. (1993c): Lithotectonic divisions of the northern part of the Torngat Orogen, Labrador, Quebec and N.W.T. In Eastern Canadian Onshore-Offshore Transect (ECSOOT), Transect Meeting (December 4-5, 1992; R.J. Wardle & J. Hall, compilers). *LITHOPROBE Rep.* **32**, 21-31.

WARDLE, R.J. (1983): Nain-Churchill province cross-section, Nachvak fiord, northern Labrador. *Newfoundland Dep. of Mines and Energy, Current Research, Rep.* **83-1**, 68-89.

_____, BRIDGWATER, D., MENGEL, F.C., CAMPBELL, L.M., VAN KRANENDONK, M.J., HAUMAN, A., CHURCHILL, R. & REID, L. (1994): Mapping in the Torngat Orogen, northernmost Labrador. Report 3. The Nain Craton (including a note on ultramafic dyke occurrences in northernmost Labrador). *Newfoundland Dep. of Mines and Energy, Geol. Surv. Branch, Rep.* **94-1**, 399-407.

_____ & VAN KRANENDONK, M.J. (1996): The eastern Churchill Province of Labrador-Québec, Canada: Orogenic development as a consequence of oblique convergence and collision. In Precambrian Crustal Evolution in the North Atlantic Region (T.S. Brewer, ed.). *Geol. Soc., Spec. Publ.* **112**, 137-154.

_____, _____, MENGEL, F. & SCOTT, D. (1992): Geological mapping in the Torngat Orogen, northernmost Labrador: preliminary results. *Newfoundland Dep. of Mines and Energy, Geol. Surv. Branch, Rep.* **92-1**, 413-429.

_____, _____, _____, _____, SCHWARZ, S. & RYAN, B. (1993): Geological mapping in the Torngat Orogen, northernmost Labrador. Report 2. *Newfoundland Dep. of Mines and Energy, Geol. Surv. Branch, Rep.* **93-1**, 77-89.

Received January 15, 1997, revised manuscript accepted July 17, 1997.

APPENDIX

Analytical details

All analyses were carried out with the JEOL 733 Superprobe housed at the Geological Institute, University of Copenhagen. The instrument was operated at an accelerating voltage of 15 kV with a beam current of 15 nA. Counting time was 20 s on peaks and 2 s on background. X-ray intensities were corrected on-line by the ZAF method, and the raw data were subsequently corrected for drift using procedures and programs developed by Jørn Rønso and Tue

Albertsen, Geological Institute. Natural and synthetic minerals were employed as standards, and were analyzed before, during and after each session.

Grains chosen for analysis in each sample were in contact or near contact (two grain diameters away). Large grains of garnet and clinopyroxene were analyzed for compositional homogeneity along traverses from rim to core. Rims of ferromagnesian minerals separated by quartz or plagioclase were generally used for determinations of "peak" P-T. Core compositions of coexisting minerals were only used in cases where reliable correlation could be made from textural observations. Where possible, several micro-

structural settings were chosen in each thin section in order to test for variable reaction-progress and to evaluate any effects due to domainal equilibrium.

Thermobarometry

In this study, thermobarometry was performed using the TWEEQU (ver. 1.02) program of Berman (1991). In all calculations, thermodynamic data for end members were taken from Berman (1988, 1990). Garnet was modeled as a mixture between Prp, Alm and Grs, with mixing properties described by Berman (1990). Plagioclase was modeled as a mixture of An and Ab, with mixing properties described by Fuhrman & Lindsley (1988). The two types of pyroxene were treated as ideal solutions. Biotite solid-solutions were modeled as end members between Ann and Phl, with the mixing model described by McMullin *et al.* (1991).

In the thermodynamic database employed (JUN92.GSC), six amphibole end-members are presently available: Tremolite (Tr), Aluminotschermakite (Ts), Pargasite (Pg) and their Fe-equivalents ferro-actinolite, alumino-ferrotschermakite and ferropargasite (nomenclature of Leake *et al.* 1997). Thermochemical data and mixing models for these end members have been determined by Mäder *et al.* (1994). These authors recommended using Fe and Mg end-members in all Grt-Hbl exchange reactions, in conjunction with Mg end-members in the net-transfer reactions. Through a number of tests, we obtained similar results (within 0.3 kbar and 25°C) by using Ts, Tr and their Fe-equivalents in both exchange and net-transfer reactions. Consequently, only these amphibole end-members were included in thermobarometric calculations with the GHPQ assemblage in this study.